(29) F. G. Mann, D. Purdie, and A. F. Wells, *J. Chem. Soc.*, 1503 (1936).
(30) M. R. Churchill and K. L. Kalra, *Inorg. Chem.*, **13**, 1899 (1974).
(31) M. R. Churchill, B. G. DeBoer, and S. J. Mendak, *Inorg. Chem.*, **14**, 2041 (1975).
(32) M. R. Churchill and K. L. Kalra, *Inorg. Chem.*, **13**, 1065 (1974).
(33) M. R. Churchill and K. L. Kalra, *Inorg. Chem.*, **13**, 1427 (1974).
(34) M. R. Churchill, B. G. DeBoer, and D. J. Donovan, *Inorg. Chem.*, **14**, 617 (1975).
(35) W. R. Clayton and S. G. Shore, *Cryst. Struct. Commun.*, **2**, 605 (1973).
(36) (a) N. Marsich, G. Nardin, and L. Randaccio, *J. Am. Chem. Soc.*, **95**, 4053 (1973); (b) G. Nardin and L. Randaccio, *Acta Crystallogr., Sect. B*, **30**, 1377 (1974); (c) A. Camus, G. Nardin, and L. Randaccio, *Inorg. Chim. Acta*, **12**, 23 (1975).
(37) F. G. Mann, A. F. Wells, and D. Purdie, *J. Chem. Soc.*, 1828 (1937).
(38) B. K. Teo and J. C. Calabrese, *J. Am. Chem. Soc.*, **97**, 1256 (1975).
(39) B. K. Teo and J. C. Calabrese, *J. Chem. Soc., Chem. Commun.*, 185 (1976).
(40) B. K. Teo and J. C. Calabrese, *Inorg. Chem.*, following paper in this issue.
(41) M. R. Churchill and B. G. Deboer, *Inorg. Chem.*, **14**, 2502 (1975).
(42) "International Tables for X-Ray Crystallography", Vol. I, 2d ed, Kynoch Press, Birmingham, England, 1965, p 149.
(43) R. A. Sparks et al., "Operations Manual. Syntex P$\bar{1}$ Diffractometer", Syntex Analytical Instruments, Cupertino, Calif., 1970.
(44) The absorption correction program DEAR (J. F. Blount) uses the Gaussian integration method of W. R. Busing and H. A. Levy, *Acta Crystallogr.*, **10**, 180 (1957).
(45) The integrated intensity (I) was calculated according to the expression $I = [S - (B_1 + B_2)/B_R]T_R$ where S is the scan counts, B_1 and B_2 are the background counts, B_R is the ratio of background time to scan time, and T_R is the 2θ scan rate in degrees per minute. The standard deviation of I was calculated as $\sigma(I) = T_R[S + (B_1 + B_2)/B_R^2 + (pI)^2]^{1/2}$.
(46) All least-squares refinements were based on the minimization of $\sum w_i||F_o| - |F_c||^2$ with the individual weights $w_i = 1/\sigma(F_o)^2$. Atomic scattering factors used for all nonhydrogen atoms are from H. P. Hanson, F. Herman, J. D. Lea, and S. Skillman, *Acta Crystallogr.*, **17**, 1040 (1964); those for the hydrogen atoms are from R. F. Stewart, E. R. Davidson, and W. T. Simpson, *J. Chem. Phys.*, **42**, 3175 (1965).
(47) Hydrogen atoms were calculated at C–H distances of 1.00 Å and assigned constant isotropic thermal parameters of 7.00 Å^2.
(48) $R_1 = [\sum||F_o| - |F_c||/\sum|F_o|] \times 100\%$ and $R_2 = [\sum w_i||F_o| - |F_c||^2/\sum w_i|F_o|^2]^{1/2} \times 100\%$. See supplementary material for a listing of observed and calculated structure factors.
(49) "International Tables for X-Ray Crystallography", Vol. III, Kynoch Press, Birmingham, England, 1962, p 215.
(50) C. K. Johnson, *J. Appl. Crystallogr.*, **6**, 318 (1973): ORTEP2.
(51) *Chem. Soc., Spec. Publ.*, **No. 18**, S3s (1965).
(52) K. Aurivillius, A. Cassel, and L. Falth, *Chem. Scr.*, **5**, 9 (1974).
(53) van der Waals radii of Cl (1.80 Å), Br (1.95 Å), I (2.15 Å), and H (1.20 Å) are taken from L Pauling, "The Nature of the Chemical Bond", 3d ed, Cornell University Press, Ithaca, N.Y., 1960, p 260.
(54) The following estimated single-bond covalent radii were taken from L. Pauling, "The Nature of the Chemical Bond", 3d ed, Cornell University Press, Ithaca, N.Y., 1960, pp 224, 256: Cl, 0.99 Å; Br, 1.14 Å; I, 1.33 Å; P, 1.10 Å; As, 1.21 Å; Cu, 1.17 Å; Ag, 1.34 Å.
(55) L. F. Dahl, E. Rodulfo de Gil, and R. D. Feltham, *J. Am. Chem. Soc.*, **91**, 1653 (1969).
(56) Using space-filling Courtauld atomic models from Griffin and Georgy Ltd., Wembley, Middlesex, England, the van der Waals volumes of an ethyl and of a phenyl group are measured to be approximately 35 and 83 Å^3, respectively.
(57) H. A. Bent, *J. Chem. Educ.*, **37**, 616 (1960).
(58) Based on an extensive ^{31}P NMR studies, the s character of Ag–P bonds for various hybridizations has been discussed by E. L. Muetterties and C. W. Alegranti, *J. Am. Chem. Soc.*, **94**, 6386 (1972).
(59) P. Kollman, *J. Am. Chem. Soc.*, **96**, 4363 (1974).
(60) B. K. Teo, M. B. Hall, R. F. Fenske, and L. F. Dahl, *Inorg. Chem.*, **14**, 3103 (1975).

Contribution from Bell Laboratories, Murray Hill, New Jersey 07974, and the Department of Chemistry, University of Wisconsin, Madison Wisconsin 53706

Stereochemical Systematics of Metal Clusters. Crystallographic Evidence for a New Cubane ⇌ Chair Isomerism in Tetrameric Triphenylphosphine Silver Iodide, $(Ph_3P)_4Ag_4I_4$

BOON-KENG TEO*[1a] and JOSEPH C. CALABRESE[1b]

Received March 26, 1976 AIC602339

The tetrameric triphenylphosphine silver iodide, obtained by the reaction of triphenylphosphine with silver iodide, has been shown by single-crystal x-ray diffraction studies to exist in either a cubane- or a chair-like structure in the solid state. Slow crystallization of this complex from chloroform/ether afforded monoclinic crystals of centrosymmetric space group $P2_1/c$ with $a = 24.991$ (5) Å, $b = 12.402$ (3) Å, $c = 25.074$ (6) Å, $\beta = 113.30$ (7)°, $V = 7137$ (3) Å^3, and $Z = 4$. A complete structural analysis, with final reliability indices of $R_1 = 4.83\%$ and $R_2 = 5.63\%$, revealed a cubane-like configuration defined by two interpenetrating silver and iodine tetrahedra situated on alternate corners of a highly distorted cube, with each silver atom being further coordinated to a triphenylphosphine ligand. The unusual degree of distortion from the idealized T_d molecular symmetry is manifest in that the silver···silver distances span from 3.115 (2) to 3.768 (2) Å (3.483 Å (average)), the iodine···iodine distances vary from 4.399 (2) to 4.801 (2) Å (4.582 Å (average)), and the silver–iodine bond lengths range from 2.836 (2) to 3.037 (2) Å (2.910 Å (average)). On the other hand, slow crystallization of $(Ph_3P)_4Ag_4I_4$ from methylene chloride/ether produced triclinic crystals of centrosymmetric space group $P\bar{1}$ with $a = 12.102$ (3) Å, $b = 15.071$ (2) Å, $c = 11.948$ (2) Å, $\alpha = 110.59$ (1)°, $\beta = 96.40$ (2)°, $\gamma = 71.64$ (2)°, $V = 1936$ (1) Å^3, and $Z = 1$ ($(Ph_3P)_4Ag_4I_4 \cdot 1.5CH_2Cl_2$). Structural analysis yielded $R_1 = 4.50\%$ and $R_2 = 6.52\%$. The molecule has a crystallographically imposed C_i-$\bar{1}$ symmetry with the Ag_4I_4 core defining a chair-like configuration. The silver···silver, iodine···iodine, and silver–iodine distances range from 3.095 (1) to 4.315 (2), 4.505 (1) to 4.763 (1), and 2.724 (1) to 2.995 (1) Å, respectively. The silver–iodine bond lengths can be correlated with the coordination numbers of the silver and/or the iodine atoms. This unprecedented type of isomerism allows a direct stereochemical comparison between the cubane and the chair configurations. The intriguing stereochemical variations of the $(R_3Y)_4M_4X_4$ (R = C_6H_5, C_2H_5; Y = P, As; M = Cu, Ag; X = Cl, Br, I) family are rationalized in terms of intramolecular van der Waals repulsions involving the bulkyl terminal ligands and the bridging halogens.

Introduction

As part of a continuing effort to elucidate *electronic*[2-9] *vs. steric*[10-14] effects in dictating the stereochemistries of tetrameric metal cluster systems possessing a M_4X_4 (M = metal; X = bridging ligand) core, we wish to report the synthesis and structural characterization of the title compound.[11a] Rather unexpectedly, we have found that $(Ph_3P)_4Ag_4I_4$ is capable of existing in both a highly distorted cubane-like configuration (I) and a chair-like structure (II) in solid state.

This unprecedented type of isomerism provides an excellent opportunity for a *direct* comparison of accurate molecular parameters of both forms which, along with other analogous

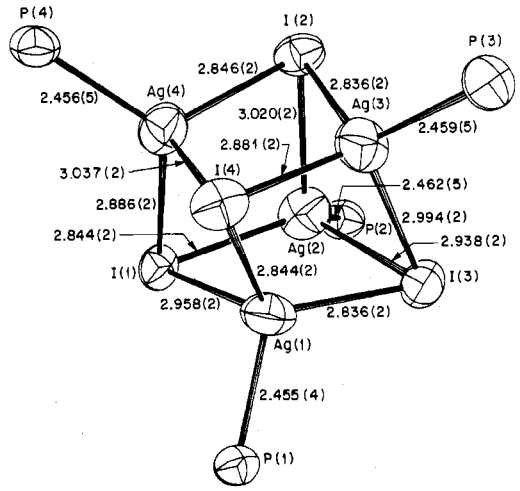

Figure 1. Highly distorted $P_4Ag_4I_4$ core of the cubane-like isomer of $(Ph_3P)_4Ag_4I_4$ (ORTEP diagram, 50% probability ellipsoids) with no crystallographic constraint.

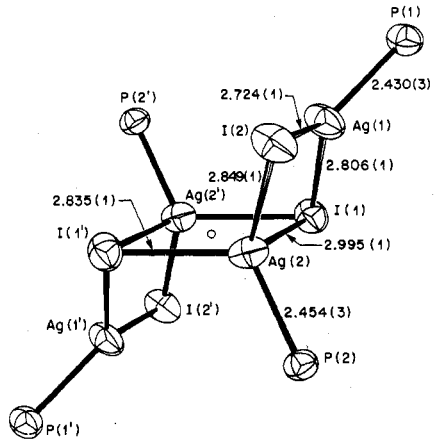

Figure 2. $P_4Ag_4I_4$ core of the chair-like isomer of $(Ph_3P)_4Ag_4I_4$ (ORTEP diagram, 50% probability ellipsoids) with crystallographic C_i-$\bar{1}$ site symmetry.

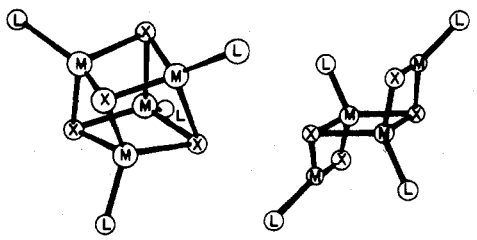

I II

silver and copper systems, enable a detailed assessment of the dominant factors causing (1) the significant distortion of the cubane-like structures of $(Ph_3P)_4Ag_4X_4$ (X = Cl, Br, I)[11] and $(Ph_3P)_4Cu_4Cl_4$,[12c] (2) the isomerization of $(Ph_3P)_4Ag_4I_4$ to give both the cubane and the chair forms, and (3) the conversion from a cubane-like structure in $(Ph_3P)_4Cu_4Cl_4$ to a chair-like configuration in $(Ph_3P)_4Cu_4X_4$ (X = Br, I).[12d,e]

Experimental Data

The compound $(Ph_3P)_4Ag_4I_4$ was prepared by reacting AgI in saturated aqueous KI solution with a stoichiometric amount of triphenylphosphine in ether under constant stirring at room temperature. The white precipitate (initially formed at the solution interface) in the ether phase was filtered, washed thoroughly with saturated KI solution, water, ethanol, and ether, and vacuum-dried. Elemental analysis (Galbraith Laboratories, Knoxville, Tenn.) suggested the stoichiometry $(C_6H_5)_3PAgI$. Anal. Calcd: C, 43.49; H, 3.04; P, 6.23; I, 25.53. Found: C, 43.51; H, 3.03; P, 6.32; I, 24.88. *Slow* crystallization of this crude product from $CHCl_3/Et_2O$ afforded crystals of monoclinic symmetry which were shown by x-ray crystallographic studies to be a cubane-like tetramer. A similar crys-

Table I

	Cubane-like	Chair-like
	(a) Crystal Data	
Formula	$[(C_6H_5)_3PAgI]_4$	$[(C_6H_5)_3PAgI]_4 \cdot 1.5\ CH_2Cl_2$
Crystal color	Colorless	Colorless
Crystal shape		
Crystal face indices, distance from centroid, mm	±(001, 0.13) ±($\bar{1}$11, 0.13) ±($\bar{1}$00, 0.18) ±(11$\bar{1}$, 0.14) ±($\bar{1}$1$\bar{1}$, 0.13) ±($\bar{1}$01, 0.18) ±(11$\bar{1}$, 0.17)	±(11$\bar{1}$, 0.07) ±(100, 0.13) ±(001, 0.16) ±(11$\bar{2}$, 0.21) (2$\bar{1}$1, 0.08) (0$\bar{1}$1, 0.16)
Cell parameters (errors)		
a, Å	24.991 (5)	12.102 (3)
b, Å	12.402 (3)	15.070 (2)
c, Å	25.074 (6)	11.948 (2)
α, deg		110.59 (1)
β, deg	113.30 (7)	96.40 (2)
γ, deg		71.64 (2)
Cell vol, Å^3	7137 (3)	1936 (1)
Z	4	1
d_{calcd}, g/cm^3	1.850	1.815
d_{obsd}, g/cm^3 (by flotation)	1.86	1.84
Laue symmetry	Monoclinic	Triclinic
Space group	$P2_1/c$ [C_{2h}^5; No. 14][15a]	$P\bar{1}$ [C_i^1; No. 2][15b]
Systematic absences	$h0l$, $l = 2n + 1$ $0k0$, $k = 2n + 1$	None
Equivalent positions	±(x, y, z) ±(x, $^1/_2 - y$, $^1/_2 + z$)	±(x, y, z)
	(b) Collection and Reduction of the X-Ray Diffraction Data	
Diffractometer	Syntex $P\bar{1}$[16]	Syntex $P\bar{1}$[16]
Radiation (graphite monochromated)	Mo Kα	Mo Kα
Range of transmission	0.52–0.55[17]	0.48–0.71[17]
μ, cm^{-1}	29.28	29.20
Takeoff angle, deg	4	4
Scan speed (limits), deg/min	2–24	4 to 24
Scan range, deg	~2	~2
Background:scan time ratio	0.67	0.67
Scan method	θ–2θ	θ–2θ
No./freq of std reflection	2/50	2/50
Intensity variation of std reflections	±4%	±2%
2θ limits, deg	2–40	2–40
Cutoff of obsd data	2$\sigma(I)$	2$\sigma(I)$
Unique data	5417[18]	3642[18]
p	0.055[18]	0.055[18]
	(c) Solution and Refinement	
Technique of solution	Heavy atom	
Method of refinement	Full-matrix least squares[19–22]	
Isotropic convergence	R_1 = 8.13%[23] R_2 = 7.97%[23]	R_1 = 11.30% R_2 = 12.35%
Isotropic-anisotropic convergence	R_1 = 4.83% R_2 = 5.63%	R_1 = 4.50% R_2 = 6.52%
Max shifts (Δ/σ)	0.04 (x, y, z) 0.07 (B) – (solvent)	0.04 (x, y, z) 0.02 (B) 0.65 (solvent)
Error of fit	1.35	1.70
Data/parameter	3774/397	2977/223
Anomalous dispersion cor		
$\Delta f'$ (real)[24]	–0.9 (Ag), 0.1 (P), –0.5 (I), 0.1 (Cl)	
$\Delta f''$ (imag)	1.4 (Ag), 0.2 (P), 2.4 (I), 0.2 (Cl)	
Max residual intensity of final diff map, e/Å^3	0.6	1.4 (near solvent); others <0.9

Table II

Positional ($\times 10^4$) and Isotropic Thermal Parameters with Esd's for $(Ph_3P)_4Ag_4I_4$ (Cubane)

Atom	x	y	z	B, Å^2	Atom	x	y	z	B, Å^2
I(1)	8 123.5 (5)	6 478.9 (9)	2062.4 (5)	*a*	C(1L)	5 453 (7)	6 545 (13)	857 (7)	5.2 (4)
I(2)	7 025.6 (5)	6 729.9 (9)	3066.8 (5)	*a*	C(2L)	5 066 (9)	6 533 (17)	286 (9)	8.0 (6)
I(3)	8 294.3 (5)	4 074.1 (10)	3511.2 (5)	*a*	C(3L)	4 513 (10)	5 929 (20)	156 (10)	9.7 (7)
I(4)	6 666.8 (5)	3 982.0 (9)	1667.4 (5)	*a*	C(4L)	4 466 (11)	5 405 (19)	596 (11)	9.7 (7)
Ag(1)	7 890.3 (6)	4 221.0 (12)	2285.3 (6)	*a*	C(5L)	4 811 (11)	5 411 (19)	1116 (10)	9.6 (7)
Ag(2)	8 282.4 (7)	6 384.7 (13)	3248.8 (6)	*a*	C(6L)	5 373 (9)	6 007 (16)	1304 (8)	7.6 (6)
Ag(3)	7 015.0 (6)	4 472.4 (11)	2881.6 (6)	*a*	C(1M)	5 962 (7)	8 691 (13)	1163 (7)	4.5 (4)
Ag(4)	6 917.6 (6)	6 369.6 (13)	1907.7 (6)	*a*	C(2M)	5 405 (9)	9 085 (17)	896 (9)	7.8 (6)
P(1)	8 446.6 (18)	3 147.5 (34)	1858.7 (19)	*a*	C(3M)	5 309 (10)	10 195 (19)	981 (10)	8.5 (6)
P(2)	9 042.6 (20)	7 397.6 (39)	4026.5 (19)	*a*	C(4M)	5 768 (10)	10 851 (18)	1269 (9)	8.7 (6)
P(3)	6 479.7 (20)	3 299.8 (38)	3291.1 (19)	*a*	C(5M)	6 292 (12)	10 470 (21)	1516 (11)	10.7 (8)
P(4)	6 150.9 (19)	7 281.8 (39)	1092.5 (19)	*a*	C(6M)	6 415 (9)	9 351 (18)	1490 (9)	7.9 (6)
C(1A)	9 225 (6)	3 175 (13)	2251 (6)	4.2 (4)	H(2A)	9 408	1 726	1940	7.0[b]
C(2A)	9 578 (8)	2 357 (14)	2198 (7)	5.8 (5)	H(3A)	10 445	1 837	2472	7.0
C(3A)	10 194 (8)	2 427 (16)	2513 (8)	7.0 (5)	H(4A)	10 842	3 312	3076	7.0
C(4A)	10 421 (8)	3 305 (16)	2848 (8)	6.5 (5)	H(5A)	10 270	4 756	3172	7.0
C(5A)	10 099 (9)	4 104 (17)	2917 (8)	7.6 (6)	H(6A)	9 230	4 588	2668	7.0
C(6A)	9 472 (8)	4 035 (15)	2605 (8)	6.3 (5)	H(2B)	8 527	1 500	1083	7.0
C(1B)	8 269 (6)	1 717 (12)	1757 (6)	4.0 (4)	H(3B)	8 333	−397	972	7.0
C(2B)	8 375 (8)	1 119 (15)	1356 (8)	6.4 (5)	H(4B)	7 964	−1 220	1580	7.0
C(3B)	8 241 (10)	−5 (20)	1289 (10)	9.6 (7)	H(5B)	7 813	−341	2320	7.0
C(4B)	8 041 (9)	−439 (18)	1656 (10)	8.6 (6)	H(6B)	8 003	1 634	2465	7.0
C(5B)	7 944 (9)	78 (19)	2060 (9)	8.8 (6)	H(2C)	9 157	4 231	1313	7.0
C(6B)	8 062 (9)	1 223 (17)	2130 (9)	7.9 (6)	H(3C)	8 881	4 924	334	7.0
C(1C)	8 335 (7)	3 597 (12)	1132 (6)	4.4 (4)	H(4C)	7 977	4 525	−390	7.0
C(2C)	8 761 (8)	4 113 (15)	1020 (8)	6.2 (5)	H(5C)	7 256	3 657	−167	7.0
C(3C)	8 597 (10)	4 500 (18)	426 (10)	9.0 (7)	H(6C)	7 480	3 082	809	7.0
C(4C)	8 064 (10)	4 305 (18)	21 (9)	8.4 (6)	H(2D)	5 852	2 852	4065	7.0
C(5C)	7 656 (10)	3 793 (17)	137 (10)	8.8 (6)	H(3D)	6 090	3 214	5064	7.0
C(6C)	7 786 (8)	3 435 (15)	703 (8)	7.0 (5)	H(4D)	6 873	4 354	5584	7.0
C(1D)	6 562 (7)	3 628 (13)	4014 (7)	4.5 (4)	H(5D)	7 560	4 805	5176	7.0
C(2D)	6 212 (9)	3 263 (17)	4295 (9)	8.4 (6)	H(6D)	7 300	4 528	4161	7.0
C(3D)	6 335 (10)	3 519 (18)	4874 (10)	8.8 (6)	H(2E)	7 365	2 189	3065	7.0
C(4D)	6 799 (10)	4 106 (19)	5166 (10)	9.1 (6)	H(3E)	7 763	345	3233	7.0
C(5D)	7 181 (11)	4 472 (20)	4937 (11)	10.4 (7)	H(4E)	7 192	−1 005	3460	7.0
C(6D)	7 045 (9)	4 237 (17)	4351 (9)	8.2 (6)	H(5E)	6 475	−497	3746	7.0
C(1E)	6 714 (7)	1 919 (13)	3335 (7)	5.1 (4)	H(6E)	6 138	1 268	3680	7.0
C(2E)	7 175 (11)	1 668 (21)	3206 (10)	10.8 (8)	H(2F)	5 505	4 690	3201	7.0
C(3E)	7 400 (13)	543 (26)	3261 (13)	13.4 (10)	H(3F)	4 481	4 579	2661	7.0
C(4E)	7 108 (11)	−205 (21)	3437 (10)	10.3 (7)	H(4F)	4 085	3 123	2147	7.0
C(5E)	6 687 (11)	41 (20)	3594 (10)	9.4 (7)	H(5F)	4 615	1 907	1883	7.0
C(6E)	6 471 (9)	1 113 (18)	3554 (9)	8.3 (6)	H(6F)	5 701	1 899	2398	7.0
C(1F)	5 702 (8)	3 255 (17)	2899 (8)	6.8 (5)	H(2H)	8 875	9 478	4455	7.0
C(2F)	5 343 (12)	4 038 (21)	2931 (11)	10.9 (8)	H(3H)	8 888	11 314	4175	7.0
C(3F)	4 714 (15)	3 939 (26)	2614 (14)	13.5 (10)	H(4H)	9 312	11 720	3466	7.0
C(4F)	4 515 (13)	3 180 (28)	2312 (14)	13.5 (10)	H(5H)	9 565	10 208	3013	7.0
C(5F)	4 821 (17)	2 481 (30)	2159 (15)	16.3 (12)	H(6H)	9 416	8 462	3256	7.0
C(6F)	5 463 (14)	2 423 (25)	2502 (13)	13.3 (9)	H(2I)	9 468	5 313	4042	7.0
C(1H)	9 134 (7)	8 781 (14)	3879 (7)	5.5 (4)	H(3I)	10 394	4 402	4400	7.0
C(2H)	9 002 (10)	9 615 (20)	4139 (10)	9.4 (7)	H(4I)	11 246	5 456	4861	7.0
C(3H)	9 049 (11)	10 725 (22)	3970 (11)	11.1 (8)	H(5I)	11 187	7 323	4952	7.0
C(4H)	9 265 (9)	10 957 (18)	3576 (9)	8.2 (6)	H(6I)	10 275	8 183	4557	7.0
C(5H)	9 410 (12)	10 113 (26)	3330 (12)	12.7 (9)	H(2J)	9 743	7 875	5235	7.0
C(6H)	9 318 (11)	9 052 (21)	3459 (11)	10.6 (7)	H(3J)	9 525	8 061	6086	7.0
C(1I)	9 765 (7)	6 835 (14)	4262 (7)	5.0 (4)	H(4J)	8 566	7 637	6015	7.0
C(2I)	9 823 (9)	5 762 (18)	4224 (9)	8.2 (6)	H(5J)	7 872	6 963	5139	7.0
C(3I)	10 379 (11)	5 200 (19)	4445 (10)	9.2 (7)	H(6J)	8 077	6 928	4306	7.0
C(4I)	10 856 (9)	5 814 (17)	4691 (8)	7.1 (5)	H(2K)	5 893	8 727	98	7.0
C(5I)	10 827 (10)	6 860 (19)	4744 (9)	8.9 (6)	H(3K)	6 109	8 682	−757	7.0
C(6I)	10 278 (9)	7 390 (17)	4509 (8)	7.8 (6)	H(4K)	6 747	7 358	−841	7.0
C(1J)	8 906 (7)	7 467 (13)	4681 (7)	4.6 (4)	H(5K)	7 116	6 024	−131	7.0
C(2J)	9 331 (9)	7 761 (16)	5200 (9)	8.0 (6)	H(6K)	6 903	6 003	713	7.0
C(3J)	9 216 (9)	7 811 (17)	5721 (9)	8.4 (6)	H(2L)	5 162	6 923	−17	7.0
C(4J)	8 661 (9)	7 566 (16)	5662 (8)	7.0 (5)	H(3L)	4 224	6 031	−304	7.0
C(5J)	8 253 (9)	7 224 (16)	5164 (9)	7.2 (5)	H(4L)	4 056	5 053	385	7.0
C(6J)	8 374 (8)	7 160 (14)	4671 (8)	6.2 (5)	H(5L)	4 659	4 945	1340	7.0
C(1K)	6 317 (7)	7 330 (14)	449 (7)	5.0 (4)	H(6L)	5 617	5 992	1712	7.0
C(2K)	6 135 (9)	8 132 (17)	44 (9)	7.8 (6)	H(2M)	5 068	8 581	696	7.0
C(3K)	6 280 (10)	8 114 (19)	−444 (10)	9.3 (7)	H(3M)	4 881	10 473	775	7.0
C(4K)	6 637 (8)	7 336 (16)	−496 (8)	7.0 (5)	H(4M)	5 673	11 614	1297	7.0
C(5K)	6 854 (7)	6 571 (15)	−92 (8)	6.1 (5)	H(5M)	6 619	10 986	1724	7.0
C(6K)	6 707 (7)	6 572 (14)	397 (7)	5.8 (5)	H(6M)	6 805	9 076	1717	7.0

Table II (*Continued*)

Anisotropic Thermal Parameters (×10⁴) with Esd's

Atom	β_{11}	β_{22}	β_{33}	β_{12}	β_{13}	β_{23}
I(1)	20.9 (2)	71.7 (10)	26.2 (3)	−3.5 (4)	9.8 (2)	10.6 (5)
I(2)	24.2 (2)	69.5 (10)	26.7 (3)	5.5 (4)	9.1 (2)	−9.9 (5)
I(3)	26.0 (3)	84.4 (11)	25.2 (3)	6.0 (5)	8.5 (2)	8.0 (5)
I(4)	22.8 (2)	81.1 (11)	27.4 (3)	−4.0 (5)	8.9 (2)	−3.1 (5)
Ag(1)	26.0 (3)	94.5 (13)	32.7 (3)	4.5 (6)	16.1 (2)	−1.5 (6)
Ag(2)	30.9 (4)	106.5 (15)	27.2 (4)	−2.6 (7)	5.7 (3)	−8.9 (7)
Ag(3)	32.6 (3)	78.6 (13)	35.5 (3)	−6.8 (6)	18.9 (2)	3.1 (6)
Ag(4)	25.4 (3)	129.6 (17)	26.2 (3)	7.0 (7)	6.9 (3)	11.4 (7)
P(1)	18.6 (9)	56.2 (38)	22.8 (9)	0.9 (16)	9.0 (7)	0.2 (17)
P(2)	25.2 (10)	84.6 (46)	21.2 (10)	1.7 (19)	9.5 (7)	−2.3 (19)
P(3)	24.1 (10)	75.8 (44)	24.1 (10)	−10.8 (18)	11.3 (7)	−3.2 (18)
P(4)	18.3 (9)	91.6 (47)	23.1 (10)	0.6 (18)	8.8 (7)	−2.6 (19)

[a] Anisotropic thermal parameters (×10⁴) of the form $\exp[-(h^2\beta_{11} + k^2\beta_{22} + l^2\beta_{33} + 2hk\beta_{12} + 2hl\beta_{13} + 2kl\beta_{23})]$ are given in the second part of this table. [b] Hydrogen atoms were calculated at C–H distances of 1.00 Å and assigned constant isotropic thermal parameters of 7.00 Å².

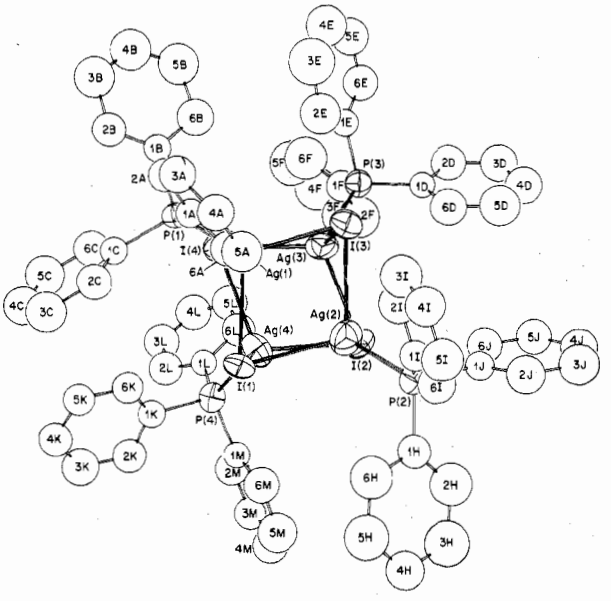

Figure 3. Stereochemistry of the cubane-like $(Ph_3P)_4Ag_4I_4$ molecule.

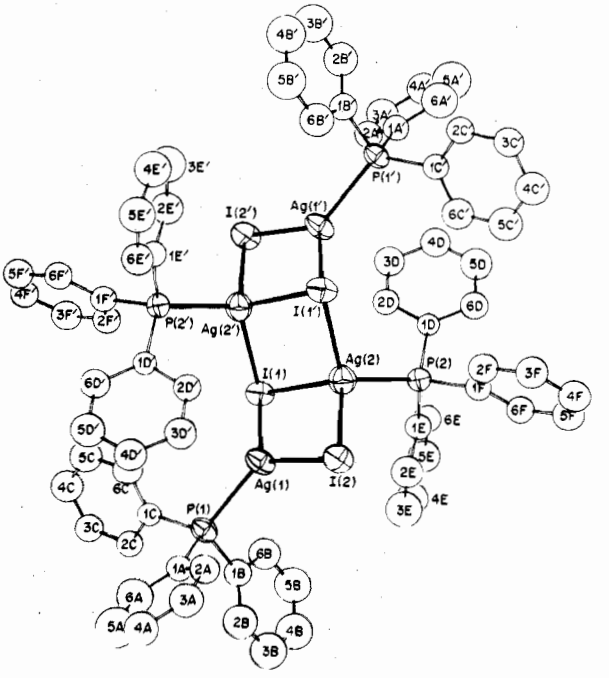

Figure 4. Stereochemistry of the chair-like $(Ph_3P)_4Ag_4I_4$ molecule.

tallization from CH_2Cl_2/Et_2O produced crystals of triclinic symmetry (along with some crystals of morphology similar to those obtained from $CHCl_3$) which were shown by structural studies to adopt a chair-like configuration.

The crystallographical details of the two phases of $(Ph_3P)_4Ag_4I_4$ are summarized in Table I.

The final positional and thermal parameters, with errors estimated from the full variance–covariance matrix, are listed in Tables II and III for the cubane and the chair isomer, respectively.

Results and Discussion

I. Description of the Structures. The two isomers of $(Ph_3P)_4Ag_4I_4$ are portrayed in Figures 1–4.[25] The cubane-like structure (Figures 1 and 3) is composed of four silver and four iodine atoms situated at alternate corners of a highly distorted cube with each silver atom being further coordinated to one triphenylphosphine ligand. The chair-like (Figures 2 and 4) configuration can be considered as derived from the cubane-like structure via cleavage of one of the six nonplanar Ag_2I_2 faces (rupture of two Ag–I bonds) followed by rotation of one adjacent Ag_2I_2 face by approximately 180°.

It is interesting to note that the cubane isomer is not isomorphous with the $(Ph_3P)_4Ag_4Cl_4$[11b] homologue (the former has a highly distorted cubane-like structure with no crystallographic constraint in $P2_1/c$ whereas the latter has a somewhat distorted cubane-like structure with crystallographic C_2-2 site symmetry in *Pbcn*); nor is the chair isomer isomorphous with its structurally analogous $(Ph_3P)_4Cu_4I_4$[12e] (the former belongs to $P\bar{1}$ whereas the latter belongs to $C2/c$; both, however, have a crystallographically imposed center of symmetry).

The crystal structures of both the cubane and the chair-like phases are composed of isolated molecules separated by van der Waals distances. The latter, however, incorporates solvent (CH_2Cl_2) of crystallization. Tables IV–VII list the pertinent intramolecular distances and bond angles for the cubane and the chair forms, respectively.

The structural characteristics of these two isomers of $(Ph_3P)_4Ag_4I_4$ can be described as follows.

Cubane-like $(Ph_3P)_4Ag_4I_4$. The most intriguing feature of this cubane-like structure is its unusual degree of distortion from the idealized T_d symmetry.

This unusual degree of *nonsystematic* distortion manifests itself in the following molecular parameters. First, the silver···silver distances span from 3.115 (2) to 3.768 (2) Å with an average of 3.483 Å. This variation of the metal···metal distance over a range of 0.65 Å is rather remarkable. Though all six Ag···Ag distances are best considered as nonbonding from electronic reasonings, the shortest one (3.115 (2) Å) is only 0.226 Å longer than the 2.889-Å value found in silver metal.[26] Second, the I···I distances vary from 4.399 (2) to

Table III

Positional ($\times 10^4$) and Isotropic Thermal Parameters with Esd's for $(Ph_3P)_4Ag_4I_4$ (Chair)

Atom	x	y	z	B, Å^2	Atom	x	y	z	B, Å^2
I(1)	3 689.1 (7)	821.0 (6)	1 617.9 (7)	*a*	H(2A)	4 504	4 451	1 386	7.0[b]
I(2)	6 539.1 (7)	2 142.5 (6)	923.3 (8)	*a*	H(3A)	4 512	5 798	793	7.0
Ag(1)	4 310.6 (8)	2 432.4 (7)	1 510.9 (9)	*a*	H(4A)	2 846	7 175	1 045	7.0
Ag(2)	6 134.3 (9)	356.6 (7)	837.3 (9)	*a*	H(5A)	1 164	7 246	1 928	7.0
P(1)	2 869.4 (27)	4 003.5 (23)	2 475.8 (29)	*a*	H(6A)	1 107	5 882	2 520	7.0
P(2)	7 349.7 (26)	−454.1 (23)	2 196.3 (27)	*a*	H(2B)	3 102	5 848	4 334	7.0
C(1A)	2 825 (10)	5 035 (9)	2 033 (10)	3.9 (2)	H(3B)	3 478	6 258	6 409	7.0
C(2A)	3 782 (11)	5 022 (10)	1 514 (12)	5.1 (3)	H(4B)	4 054	5 063	7 277	7.0
C(3A)	3 791 (13)	5 828 (11)	1 155 (13)	6.3 (3)	H(5B)	3 778	3 502	6 316	7.0
C(4A)	2 834 (14)	6 605 (12)	1 297 (14)	7.0 (4)	H(6B)	3 343	3 017	4 178	7.0
C(5A)	1 869 (16)	6 663 (13)	1 821 (16)	8.6 (4)	H(2C)	772	5 006	4 026	7.0
C(6A)	1 831 (15)	5 865 (13)	2 183 (15)	8.1 (4)	H(3C)	−1 158	4 878	3 720	7.0
C(1B)	3 175 (10)	4 400 (9)	4 064 (11)	4.7 (3)	H(4C)	−1 727	3 849	1 909	7.0
C(2B)	3 231 (13)	5 334 (12)	4 720 (14)	6.9 (4)	H(5C)	−321	2 861	378	7.0
C(3B)	3 513 (16)	5 574 (15)	5 935 (18)	9.0 (5)	H(6C)	1 649	2 907	667	7.0
C(4B)	3 760 (15)	4 908 (14)	6 447 (16)	8.4 (4)	H(2D)	5 622	−1 429	1 373	7.0
C(5B)	3 683 (15)	3 967 (14)	5 858 (17)	8.5 (4)	H(3D)	5 544	−3 086	871	7.0
C(6B)	3 392 (13)	3 690 (11)	4 614 (14)	6.5 (3)	H(4D)	7 224	−4 358	1 140	7.0
C(1C)	1 376 (9)	3 961 (8)	2 361 (10)	3.6 (2)	H(5D)	8 995	−3 973	1 786	7.0
C(2C)	557 (10)	4 530 (9)	3 251 (11)	4.4 (3)	H(6D)	9 069	−2 311	2 327	7.0
C(3C)	−579 (11)	4 455 (10)	3 040 (12)	5.2 (3)	H(2E)	6 846	1 531	3 639	7.0
C(4C)	−903 (13)	3 855 (11)	2 005 (14)	6.3 (3)	H(3E)	6 161	2 499	5 656	7.0
C(5C)	−91 (13)	3 293 (11)	1 133 (14)	6.8 (4)	H(4E)	5 801	1 673	6 858	7.0
C(6C)	1 057 (12)	3 330 (10)	1 290 (13)	5.7 (3)	H(5E)	6 185	−48	6 205	7.0
C(1D)	7 357 (9)	−1 738 (8)	1 879 (9)	3.2 (2)	H(6E)	6 858	−1 000	4 195	7.0
C(2D)	6 333 (10)	−1 963 (9)	1 460 (11)	4.5 (3)	H(2F)	8 847	−677	391	7.0
C(3D)	6 273 (12)	−2 917 (10)	1 182 (12)	5.5 (3)	H(3F)	10 879	−813	306	7.0
C(4D)	7 260 (13)	−3 650 (11)	1 334 (13)	6.2 (3)	H(4F)	12 055	−732	2 036	7.0
C(5D)	8 273 (13)	−3 426 (11)	1 728 (13)	6.4 (3)	H(5F)	11 266	−594	3 832	7.0
C(6D)	8 343 (11)	−2 463 (10)	2 006 (11)	5.0 (3)	H(6F)	9 258	−444	3 958	7.0
C(1E)	6 888 (10)	193 (9)	3 758 (10)	4.0 (3)					
C(2E)	6 702 (12)	1 190 (11)	4 173 (13)	6.0 (3)					
C(3E)	6 311 (14)	1 750 (12)	5 353 (15)	7.6 (4)					
C(4E)	6 095 (13)	1 281 (12)	6 023 (14)	7.0 (4)					
C(5E)	6 272 (13)	301 (12)	5 676 (15)	7.2 (4)					
C(6E)	6 713 (12)	−268 (10)	4 484 (12)	5.5 (3)					
C(1F)	8 873 (10)	−537 (8)	2 195 (10)	3.8 (2)					
C(2F)	9 343 (11)	−648 (9)	1 118 (11)	4.9 (3)					
C(3F)	10 520 (12)	−721 (10)	1 069 (13)	5.9 (3)					
C(4F)	11 209 (11)	−693 (10)	2 058 (12)	5.3 (3)					
C(5F)	10 765 (12)	−613 (10)	3 112 (13)	5.7 (3)					
C(6F)	9 572 (11)	−526 (9)	3 183 (11)	4.7 (3)					
Cl(1)	800 (21)	2 569 (18)	5 030 (22)	12.6 (7)[c]					
Cl(2)	700 (20)	2 065 (17)	3 668 (21)	12.5 (6)					
Cl(3)	−755 (15)	2 228 (13)	4 860 (18)	11.6 (5)					
Cl(4)	−735 (16)	2 031 (14)	3 223 (20)	12.3 (5)					
Cl(5)	1 312 (17)	2 624 (14)	4 862 (16)	9.0 (5)					
Cl(6)	−852 (28)	2 227 (25)	4 006 (38)	3.2 (7)					

Anisotropic Thermal Parameters ($\times 10^4$) with Esd's

Atom	β_{11}	β_{22}	β_{33}	β_{12}	β_{13}	β_{23}
I(1)	87.6 (9)	55.0 (6)	83.9 (9)	−23.8 (6)	16.5 (6)	18.7 (6)
I(2)	78.2 (9)	55.0 (6)	129.1 (11)	−21.4 (6)	23.5 (7)	25.8 (6)
Ag(1)	82.1 (10)	53.7 (7)	109.2 (12)	−5.5 (6)	29.8 (8)	19.2 (7)
Ag(2)	101.8 (11)	61.7 (8)	94.6 (11)	−15.6 (7)	−10.5 (8)	37.9 (7)
P(1)	63.8 (28)	45.8 (21)	84.9 (33)	−9.3 (19)	16.2 (24)	20.6 (22)
P(2)	64.1 (28)	49.4 (21)	64.7 (30)	−16.0 (19)	−0.0 (22)	22.8 (21)

[a] Anisotropic thermal parameters ($\times 10^4$) of the form $\exp[-(h^2\beta_{11} + k^2\beta_{22} + l^2\beta_{33} + 2hk\beta_{12} + 2hl\beta_{13} + 2kl\beta_{23})]$ are given in the second part of this table. [b] Hydrogen atoms were calculated at C–H distance of 1.00 Å and assigned constant isotropic thermal parameters of 7.00 Å^2. [c] The six partial chlorine atoms found in the difference map were first assigned constant isotropic thermal parameters of 8.00 Å^2 and their weights were refined: Cl(1), 0.329; Cl(2), 0.302; Cl(3), 0.359; Cl(4), 0.365; Cl(5), 0.327; Cl(6), 0.089. Their thermal parameters were then refined to these values by holding the weights constant.

4.801 (2) Å, averaging 4.582 Å. All of these nonbonded I···I contacts are close to or greater than twice the van der Waals radius of iodine (4.30 Å),[27] indicating the relative importance of the iodine···iodine repulsions in dictating the stereochemistry. For each nonplanar Ag_2I_2 moiety, short I···I contacts are generally accompanied by long Ag···Ag distances and vice versa. Third, the Ag–I bond lengths range from 2.836 (2) to 3.037 (2) Å with a mean of 2.910 Å. These values are all substantially greater than normal covalent Ag–I bond lengths (viz., 2.67 Å) but comparable to those of 2.80, 2.77–3.00, 2.759 (6)–3.092 (7), 2.81 (1)–2.94 (1), and 2.72 (3)–3.14 (1) Å found in zinc blende type AgI,[29a] $Me_4NAg_2I_3$,[29b] $Bu_4N[Ag_3I_4]$,[29c] $RbAg_4I_5$,[29d] and $[Me_4N]_2Ag_{13}I_{15}$,[29e] respectively.

Further definitive evidence concerning the large deformation of the Ag_4I_4 core is given by the Ag–I–Ag angles ranging from 64.53 (4) to 81.07 (5)° (73.55° (average)), while the I–Ag–I angles vary from 95.16 (5) to 115.38 (5)° (104.08° (average)). The two highly acute Ag(1)–I(i)–Ag(3) angles of 64.53 (4) (i = 3) and 65.93 (5)° (i = 4), which correspond to the *shortest* Ag(1)···Ag(3) contacts, are especially remarkable for

Table IV. Interatomic Distances (Å) with Esd's for $(Ph_3P)_4Ag_4I_4$ (Cubane)

	A. Ag···Ag Distances		
Ag(1)···Ag(2)	3.4819 (21)	Ag(2)···Ag(3)	3.7678 (20)
Ag(1)···Ag(3)	3.1153 (19)	Ag(2)···Ag(4)	3.7238 (20)
Ag(1)···Ag(4)	3.4765 (20)	Ag(3)···Ag(4)	3.3298 (20)
	B. I···I Distances		
I(1)···I(2)	4.4086 (16)	I(2)···I(3)	4.3985 (16)
I(1)···I(3)	4.5877 (16)	I(2)···I(4)	4.7161 (16)
I(1)···I(4)	4.5794 (15)	I(3)···I(4)	4.8014 (17)
	C. I-Ag Bond Lengths		
I(1)-Ag(1)	2.9582 (18)	I(3)-Ag(1)	2.8364 (18)
I(1)-Ag(2)	2.8437 (18)	I(3)-Ag(2)	2.9376 (20)
I(1)-Ag(4)	2.8857 (18)	I(3)-Ag(3)	2.9939 (19)
I(2)-Ag(2)	3.0202 (19)	I(4)-Ag(1)	2.8444 (18)
I(2)-Ag(3)	2.8364 (18)	I(4)-Ag(3)	2.8810 (19)
I(2)-Ag(4)	2.8458 (18)	I(4)-Ag(4)	3.0372 (20)
	D. Ag-P Bond Lengths		
Ag(1)-P(1)	2.4546 (44)	Ag(3)-P(3)	2.4589 (45)
Ag(2)-P(2)	2.4616 (48)	Ag(4)-P(4)	2.4559 (47)
	E. P-C Bond Lengths		
P(1)-C(1A)	1.799 (15)	P(3)-C(1D)	1.790 (16)
P(1)-C(1B)	1.822 (16)	P(3)-C(1E)	1.799 (17)
P(1)-C(1C)	1.818 (15)	P(3)-C(1F)	1.798 (19)
P(2)-C(1H)	1.788 (18)	P(4)-C(1K)	1.818 (16)
P(2)-C(1I)	1.804 (16)	P(4)-C(1L)	1.847 (16)
P(2)-C(1J)	1.807 (16)	P(4)-C(1M)	1.836 (16)
	F. C-C Bond Lengths		
C(1A)-C(2A)	1.386 (21)	C(1F)-C(2F)	1.346 (27)
C(2A)-C(3A)	1.427 (22)	C(2F)-C(3F)	1.460 (34)
C(3A)-C(4A)	1.355 (22)	C(3F)-C(4F)	1.187 (35)
C(4A)-C(5A)	1.329 (23)	C(4F)-C(5F)	1.310 (38)
C(5A)-C(6A)	1.451 (23)	C(5F)-C(6F)	1.493 (37)
C(1A)-C(6A)	1.369 (21)	C(1F)-C(6F)	1.393 (30)
C(1B)-C(2B)	1.357 (20)	C(1H)-C(2H)	1.330 (24)
C(2B)-C(3B)	1.428 (27)	C(2H)-C(3H)	1.458 (30)
C(3B)-C(4B)	1.323 (26)	C(3H)-C(4H)	1.331 (27)
C(4B)-C(5B)	1.301 (26)	C(4H)-C(5H)	1.335 (30)
C(5B)-C(6B)	1.447 (26)	C(5H)-C(6H)	1.396 (32)
C(1B)-C(6B)	1.379 (22)	C(1H)-C(6H)	1.348 (26)
C(1C)-C(2C)	1.363 (20)	C(1I)-C(2I)	1.346 (24)
C(2C)-C(3C)	1.460 (24)	C(2I)-C(3I)	1.453 (27)
C(3C)-C(4C)	1.340 (26)	C(3I)-C(4I)	1.342 (25)
C(4C)-C(5C)	1.328 (26)	C(4I)-C(5I)	1.309 (25)
C(5C)-C(6C)	1.395 (24)	C(5I)-C(6I)	1.422 (25)
C(1C)-C(6C)	1.384 (21)	C(1I)-C(6I)	1.368 (23)
C(1D)-C(2D)	1.396 (23)	C(1J)-C(2J)	1.364 (22)
C(2D)-C(3D)	1.395 (25)	C(2J)-C(3J)	1.447 (25)
C(3D)-C(4D)	1.319 (26)	C(3J)-C(4J)	1.371 (24)
C(4D)-C(5D)	1.372 (28)	C(4J)-C(5J)	1.331 (22)
C(5D)-C(6D)	1.402 (27)	C(5J)-C(6J)	1.386 (22)
C(1D)-C(6D)	1.391 (22)	C(1J)-C(6J)	1.372 (21)
C(1E)-C(2E)	1.351 (26)	C(1K)-C(2K)	1.366 (22)
C(2E)-C(3E)	1.489 (33)	C(2K)-C(3K)	1.409 (25)
C(3E)-C(4E)	1.359 (32)	C(3K)-C(4K)	1.353 (25)
C(4E)-C(5E)	1.296 (28)	C(4K)-C(5K)	1.337 (22)
C(5E)-C(6E)	1.423 (28)	C(5K)-C(6K)	1.410 (21)
C(1E)-C(6E)	1.392 (23)	C(1K)-C(6K)	1.399 (21)
C(1L)-C(2L)	1.376 (22)	C(1M)-C(2M)	1.374 (22)
C(2L)-C(3L)	1.491 (27)	C(2M)-C(3M)	1.428 (26)
C(3L)-C(4L)	1.325 (27)	C(3M)-C(4M)	1.357 (26)
C(4L)-C(5L)	1.245 (26)	C(4M)-C(5M)	1.297 (28)
C(5L)-C(6L)	1.489 (27)	C(5M)-C(6M)	1.428 (28)
C(1L)-C(6L)	1.385 (22)	C(1M)-C(6M)	1.375 (22)

nonbonding metal···metal separation in that normally such acute bridging angles occur in metal–metal bonded M_2X_2 systems only.[30]

Despite the severe distortion of the cubane core, the four silver–phosphorus bonds fall into the small range of 2.455 (4)–2.462 (5) Å with an average of 2.458 Å which is close to the sum of covalent radii of 2.44 Å.[28] The P–Ag–I and P–Ag···Ag angles, however, are highly irregular; they range from 104.1 (1) to 123.5 (1)° (114.1° (average)) and from 131.9 (1) to 152.8 (1)° (144.2° (average)), respectively.

The unusual distortions of the Ag_4I_4 core and the highly irregular angular deformations involving the phosphine ligands point to steric overcrowding among the ligands. This latter effect is borne out by a detailed examination of intra- as well as intermolecular van der Waals contacts tabulated in Table VIII. It is apparent that the closest nonbonding (Ph)H···H(Ph) and (Ph)H···I contacts are either close to or somewhat shorter than the sum of van der Waals radii—viz., H···H = 2.40 Å and H···I = 3.35 Å.[27] These close van der Waals contacts suggest that the observed molecular deformation is the result of the packing of the bulky triphenylphosphine ligands within each molecule and the arrangement of the molecules in the crystal.

The four triphenylphosphine ligands appear to be normal. The 12 independent phosphorus–carbon bond lengths range from 1.788 (18) to 1.847 (16) Å, averaging 1.811 Å. There appears to be a correlation between the Ag–P and P–C bond lengths in that phosphine ligands with shorter Ag–P bonds contain longer P–C bonds (cf. Table IV). These differences, however, are of only marginal significance.

The 72 independent carbon–carbon bond distances span a range of 1.187 (35)–1.491 (27) Å with an average of 1.377 Å. The 12 Ag–P–C angles, ranging from 111.7 (6) to 120.3 (6)° (average 114.5°), are all greater than the ideal tetrahedral angle whereas the 12 C–P–C angles, ranging from 102.2 (7) to 105.0 (9)° (average 103.9°), are all somewhat smaller than the ideal tetrahedral value. An interesting pattern is also observed for the 24 P–C–C angles (cf. Table V); viz., those oriented toward the pseudo-threefold axis of the triphenylphosphine are somewhat greater than the ideal trigonal angle (121.5 (14)–126.4 (14)°) whereas those oriented otherwise are somewhat smaller (113.6 (14)–120.7 (17)°). We believe that this signifies the weak intratriphenylphosphine phenyl···phenyl repulsions among the "inner" hydrogens—H(2A), H(2B), H(2C) in $Ph_3P(1)$; H(2D), H(6E), H(2F) in $Ph_3P(3)$; H(2H), H(6I), H(2J) in $Ph_3P(2)$; and H(2K), H(2L), H(2M) in $Ph_3P(4)$ (cf. Table VIIIA).

Chair-like $(Ph_3P)_4Ag_4I_4$. The centrosymmetric chair-like structure of $(Ph_3P)_4Ag_4I_4$ is defined by three Ag_2I_2 moieties (as opposed to six in the cubane-like isomer): the strictly planar Ag(2)I(1)Ag(2)′I(1)′ and the nonplanar Ag(1)I(2)-Ag(2)I(1) and Ag(1)′I(2)′Ag(2)′I(1)′. These latter two Ag_2I_2 fragments are related by the crystallographically imposed center of symmetry located at the centroid of the former Ag_2I_2 plane. The four silver atoms, the four iodine atoms, and likewise the four phosphorus atoms are also required to be precisely coplanar by the crystallographic center of symmetry.

The most important feature of this as well as other chair-like structures[12d,e,14] is that the core atoms have variable coordination numbers (CN). It is evident from Figure 2 that Ag(1) and Ag(1)′ are approximately trigonal-coordinated (CN = 3) while Ag(2) and Ag(2)′ are approximately tetrahedral-coordinated (CN = 4). Similarly, I(2) and I(2)′ are doubly bridging (CN = 2) while I(1) and I(1)′ are triply bridging (CN = 3).

As was pointed out by Churchill and co-workers[12d,e] for the Cu_4X_4 core of $(Ph_3P)_4Cu_4X_4$ (X = Br, I), the 10 Ag–I bond lengths in $(Ph_3P)_4Ag_4I_4$ (chair) exhibit a systematic trend according to the coordination numbers. Thus, within Ag(1)I(2)Ag(2)I(1) and Ag(1)′I(2)′Ag(2)′I(1)′, in order of increasing coordination numbers, the Ag(m − 2)–I(4 − n) = Ag(m − 2)′–I(4 − n)′ bond lengths increase as 2.724 (1), 2.806 (1), 2.849 (1), 2.995 (1) Å for (m, n) = (3, 2), (3, 3), (4, 2), (4, 3), respectively, where m and n are coordination numbers of the silver and iodine atoms. The remaining two Ag(2)–I(1)′ = Ag(2)′–I(1) distances within the Ag(2)I(1)Ag(2)′I(1)′ plane

Table V. Bond Angles (deg) with Esd's for $(Ph_3P)_4Ag_4I_4$ (Cubane)

	A. Ag-I-Ag Angles		
Ag(1)-I(1)-Ag(2)	73.73 (5)	Ag(1)-I(3)-Ag(2)	74.15 (5)
Ag(1)-I(1)-Ag(4)	73.00 (5)	Ag(1)-I(3)-Ag(3)	64.53 (4)
Ag(2)-I(1)-Ag(4)	81.07 (5)	Ag(2)-I(3)-Ag(3)	78.87 (5)
Ag(2)-I(2)-Ag(3)	80.01 (5)	Ag(1)-I(4)-Ag(3)	65.93 (5)
Ag(2)-I(2)-Ag(4)	78.75 (5)	Ag(1)-I(4)-Ag(4)	72.38 (5)
Ag(3)-I(2)-Ag(4)	71.75 (5)	Ag(3)-I(4)-Ag(4)	68.42 (5)
	B. I-Ag-I Angles		
I(1)-Ag(1)-I(3)	104.67 (6)	I(2)-Ag(3)-I(3)	97.91 (5)
I(1)-Ag(1)-I(4)	104.20 (5)	I(2)-Ag(3)-I(4)	111.15 (6)
I(3)-Ag(1)-I(4)	115.38 (5)	I(3)-Ag(3)-I(4)	109.61 (5)
I(1)-Ag(2)-I(2)	97.45 (5)	I(1)-Ag(4)-I(2)	100.56 (5)
I(1)-Ag(2)-I(3)	105.03 (6)	I(1)-Ag(4)-I(4)	101.25 (6)
I(2)-Ag(2)-I(3)	95.16 (5)	I(2)-Ag(4)-I(4)	106.53 (6)
	C. P-Ag-I Angles		
I(1)-Ag(1)-P(1)	104.07 (11)	I(2)-Ag(3)-P(3)	119.13 (12)
I(3)-Ag(1)-P(1)	114.67 (12)	I(3)-Ag(3)-P(3)	109.04 (12)
I(4)-Ag(1)-P(1)	112.22 (11)	I(4)-Ag(3)-P(3)	109.25 (12)
I(1)-Ag(2)-P(2)	123.53 (12)	I(1)-Ag(4)-P(4)	121.31 (12)
I(2)-Ag(2)-P(2)	118.55 (12)	I(4)-Ag(4)-P(4)	104.60 (12)
I(3)-Ag(2)-P(2)	112.58 (13)	I(2)-Ag(4)-P(4)	120.35 (12)
	D. P-Ag···Ag Angles		
P(1)-Ag(1)···Ag(2)	131.91 (11)	P(3)-Ag(3)···Ag(1)	137.95 (13)
P(1)-Ag(1)···Ag(3)	152.83 (12)	P(3)-Ag(3)···Ag(2)	144.48 (12)
P(1)-Ag(1)···Ag(4)	138.81 (12)	P(3)-Ag(3)···Ag(4)	146.11 (13)
P(2)-Ag(2)···Ag(1)	149.33 (13)	P(4)-Ag(4)···Ag(1)	144.20 (12)
P(2)-Ag(2)···Ag(3)	145.64 (12)	P(4)-Ag(4)···Ag(2)	152.09 (13)
P(2)-Ag(2)···Ag(4)	149.56 (13)	P(4)-Ag(4)···Ag(3)	137.95 (12)
	E. Ag-P-C Angles		
Ag(1)-P(1)-C(1A)	115.27 (52)	Ag(3)-P(3)-C(1D)	115.18 (55)
Ag(1)-P(1)-C(1B)	116.13 (52)	Ag(3)-P(3)-C(1E)	111.74 (58)
Ag(1)-P(1)-C(1C)	112.43 (51)	Ag(3)-P(3)-C(1F)	116.0 (6)
Ag(2)-P(2)-C(1H)	116.58 (59)	Ag(4)-P(4)-C(1K)	112.14 (56)
Ag(2)-P(2)-C(1I)	114.89 (58)	Ag(4)-P(4)-C(1L)	111.41 (56)
Ag(2)-P(2)-C(1J)	112.34 (55)	Ag(4)-P(4)-C(1M)	120.26 (55)
	F. C-P-C Angles		
C(1A)-P(1)-C(1B)	104.2 (7)	C(1D)-P(3)-C(1E)	104.5 (8)
C(1A)-P(1)-C(1C)	104.3 (7)	C(1D)-P(3)-C(1F)	103.2 (8)
C(1B)-P(1)-C(1C)	103.1 (7)	C(1E)-P(3)-C(1F)	105.0 (9)
C(1H)-P(2)-C(1I)	104.2 (8)	C(1K)-P(4)-C(1L)	104.5 (7)
C(1H)-P(2)-C(1J)	103.1 (8)	C(1K)-P(4)-C(1M)	102.2 (7)
C(1I)-P(2)-C(1J)	104.2 (7)	C(1L)-P(4)-C(1M)	104.8 (7)
	G. P-C-C Angles		
P(1)-C(1A)-C(2A)	121.7 (13)	P(2)-C(1H)-C(2H)	124.7 (16)
P(1)-C(1A)-C(6A)	118.9 (13)	P(2)-C(1H)-C(6H)	120.7 (17)
P(1)-C(1B)-C(2B)	121.8 (13)	P(2)-C(1I)-C(2I)	118.8 (15)
P(1)-C(1B)-C(6B)	118.3 (14)	P(2)-C(1I)-C(6I)	126.2 (15)
P(1)-C(1C)-C(2C)	121.9 (13)	P(2)-C(1J)-C(2J)	121.5 (14)
P(1)-C(1C)-C(6C)	116.6 (13)	P(2)-C(1J)-C(6J)	120.0 (13)
P(3)-C(1D)-C(2D)	126.4 (14)	P(4)-C(1K)-C(2K)	124.0 (14)
P(3)-C(1D)-C(6D)	117.5 (13)	P(4)-C(1K)-C(6K)	118.3 (13)
P(3)-C(1E)-C(2E)	119.5 (17)	P(4)-C(1L)-C(2L)	121.6 (14)
P(3)-C(1E)-C(6E)	121.7 (14)	P(4)-C(1L)-C(6L)	113.6 (14)
P(3)-C(1F)-C(2F)	123.1 (19)	P(4)-C(1M)-C(2M)	122.7 (14)
P(3)-C(1F)-C(6F)	118.7 (20)	P(4)-C(1M)-C(6M)	116.2 (14)
	H. C-C-C Angles		
C(2A)-C(1A)-C(6A)	119.4 (15)	C(2H)-C(1H)-C(6H)	114.5 (20)
C(1A)-C(2A)-C(3A)	119.4 (16)	C(1H)-C(2H)-C(3H)	121.9 (22)
C(2A)-C(3A)-C(4A)	119.1 (17)	C(2H)-C(3H)-C(4H)	121.5 (25)
C(3A)-C(4A)-C(5A)	123.7 (19)	C(3H)-C(4H)-C(5H)	115.8 (25)
C(4A)-C(5A)-C(6A)	117.7 (19)	C(4H)-C(5H)-C(6H)	122.2 (26)
C(1A)-C(6A)-C(5A)	120.7 (17)	C(1H)-C(6H)-C(5H)	123.7 (25)
C(2B)-C(1B)-C(6B)	119.7 (16)	C(2I)-C(1I)-C(6I)	115.0 (18)
C(1B)-C(2B)-C(3B)	121.0 (18)	C(1I)-C(2I)-C(3I)	124.1 (20)
C(2B)-C(3B)-C(4B)	116.8 (22)	C(2I)-C(3I)-C(4I)	116.3 (21)
C(3B)-C(4B)-C(5B)	125.4 (24)	C(3I)-C(4I)-C(5I)	122.3 (22)
C(4B)-C(5B)-C(6B)	119.2 (22)	C(4I)-C(5I)-C(6I)	120.0 (21)
C(1B)-C(6B)-C(5B)	117.8 (19)	C(1I)-C(6I)-C(5I)	122.1 (20)
C(2C)-C(1C)-C(6C)	121.4 (16)	C(2J)-C(1J)-C(6J)	118.4 (16)
C(1C)-C(2C)-C(3C)	116.0 (17)	C(1J)-C(2J)-C(3J)	121.0 (19)
C(2C)-C(3C)-C(4C)	120.5 (20)	C(2J)-C(3J)-C(4J)	116.5 (19)
C(3C)-C(4C)-C(5C)	122.6 (22)	C(3J)-C(4J)-C(5J)	122.7 (19)

Table V (*Continued*)

H. C-C-C Angles (*Continued*)

C(4C)-C(5C)-C(6C)	119.0 (21)	C(4J)-C(5J)-C(6J)	119.9 (19)
C(1C)-C(6C)-C(5C)	120.4 (18)	C(1J)-C(6J)-C(5J)	121.3 (17)
C(2D)-C(1D)-C(6D)	115.9 (17)	C(2K)-C(1K)-C(6K)	117.3 (16)
C(1D)-C(2D)-C(3D)	121.7 (19)	C(1K)-C(2K)-C(3K)	120.7 (20)
C(2D)-C(3D)-C(4D)	119.1 (22)	C(2K)-C(3K)-C(4K)	120.0 (21)
C(3D)-C(4D)-C(5D)	123.7 (24)	C(3K)-C(4K)-C(5K)	121.2 (19)
C(4D)-C(5D)-C(6D)	116.6 (23)	C(4K)-C(5K)-C(6K)	119.4 (17)
C(1D)-C(6D)-C(5D)	122.8 (20)	C(1K)-C(6K)-C(5K)	120.9 (16)
C(2E)-C(1E)-C(6E)	118.5 (19)	C(2L)-C(1L)-C(6L)	124.8 (17)
C(1E)-C(2E)-C(3E)	121.3 (24)	C(1L)-C(2L)-C(3L)	116.2 (19)
C(2E)-C(3E)-C(4E)	115.9 (28)	C(2L)-C(3L)-C(4L)	116.4 (22)
C(3E)-C(4E)-C(5E)	122.9 (28)	C(3L)-C(4L)-C(5L)	128.1 (27)
C(4E)-C(5E)-C(6E)	122.0 (24)	C(4L)-C(5L)-C(6L)	120.7 (23)
C(1E)-C(6E)-C(5E)	119.0 (20)	C(1L)-C(6L)-C(5L)	113.7 (18)
C(2F)-C(1F)-C(6F)	118.0 (22)	C(2M)-C(1M)-C(6M)	121.0 (17)
C(1F)-C(2F)-C(3F)	120.5 (25)	C(1M)-C(2M)-C(3M)	117.9 (19)
C(2F)-C(3F)-C(4F)	120.2 (33)	C(2M)-C(3M)-C(4M)	120.1 (21)
C(3F)-C(4F)-C(5F)	124.5 (38)	C(3M)-C(4M)-C(5M)	121.0 (24)
C(4F)-C(5F)-C(6F)	118.7 (33)	C(4M)-C(5M)-C(6M)	121.9 (24)
C(1F)-C(6F)-C(5F)	115.9 (28)	C(1M)-C(6M)-C(5M)	117.6 (20)

Table VI. Interatomic Distances (Å) with Esd's for $(Ph_3P)_4Ag_4I_4$ (Chair)

A. Ag···Ag Distances

Ag(1)···Ag(2)	3.0953 (13)	Ag(2)···Ag(2)′	3.4378 (21)
Ag(1)···Ag(2)′	4.3154 (15)		

B. I···I Distances

I(1)···I(1)′	4.7116 (16)	I(1)···I(2)′	4.5047 (12)
I(1)···I(2)	4.7625 (12)		

C. Ag-I Bond Lengths

I(1)-Ag(1)	2.8055 (13)	I(2)-Ag(1)	2.7244 (12)
I(1)-Ag(2)	2.9948 (13)	I(2)-Ag(2)	2.8493 (13)
I(1)-Ag(2)′	2.8354 (14)		

D. Ag-P Bond Lengths

Ag(1)-P(1)	2.4297 (31)	Ag(2)-P(2)	2.4542 (31)

E. P-C Bond Lengths

P(1)-C(1A)	1.793 (12)	P(2)-C(1D)	1.834 (11)
P(1)-C(1B)	1.811 (13)	P(2)-C(1E)	1.831 (12)
P(1)-C(1C)	1.817 (11)	P(2)-C(1F)	1.808 (12)

F. C-C Bond Lengths

C(1A)-C(2A)	1.366 (17)	C(1D)-C(2D)	1.381 (15)
C(2A)-C(3A)	1.428 (18)	C(2D)-C(3D)	1.381 (17)
C(3A)-C(4A)	1.338 (19)	C(3D)-C(4D)	1.394 (18)
C(4A)-C(5A)	1.350 (22)	C(4D)-C(5D)	1.364 (18)
C(5A)-C(6A)	1.430 (22)	C(5D)-C(6D)	1.399 (18)
C(1A)-C(6A)	1.409 (19)	C(1D)-C(6D)	1.376 (15)
C(1B)-C(2B)	1.368 (18)	C(1E)-C(2E)	1.356 (17)
C(2B)-C(3B)	1.397 (22)	C(2E)-C(3E)	1.409 (20)
C(3B)-C(4B)	1.293 (22)	C(3E)-C(4E)	1.331 (20)
C(4B)-C(5B)	1.372 (23)	C(4E)-C(5E)	1.337 (20)
C(5B)-C(6B)	1.430 (21)	C(5E)-C(6E)	1.440 (19)
C(1B)-C(6B)	1.388 (18)	C(1E)-C(6E)	1.356 (17)
C(1C)-C(2C)	1.381 (16)	C(1F)-C(2F)	1.400 (16)
C(2C)-C(3C)	1.402 (16)	C(2F)-C(3F)	1.400 (18)
C(3C)-C(4C)	1.352 (18)	C(3F)-C(4F)	1.365 (17)
C(4C)-C(5C)	1.361 (20)	C(4F)-C(5F)	1.375 (18)
C(5C)-C(6C)	1.397 (19)	C(5F)-C(6F)	1.417 (17)
C(1C)-C(6C)	1.399 (17)	C(1F)-C(6F)	1.372 (15)

G. CH_2Cl_2 Bond Lengths

Cl(2)-Cl(1)	1.54 (3)	Cl(2)-Cl(6)	1.89 (4)
Cl(2)-Cl(4)	1.77 (3)	Cl(4)-Cl(6)	0.89 (4)
Cl(3)-Cl(4)	1.87 (3)	Cl(1)-Cl(5)	0.71 (3)
Cl(2)-Cl(5)	1.61 (3)	Cl(3)-Cl(6)	1.01 (4)

are 2.835 (1) Å, lying between the last two values and corresponding to m, n = 4, 3.

The five silver···silver distances vary substantially from Ag(1)···Ag(2) = Ag(1)′···Ag(2)′ = 3.095 (1) to Ag(2)···Ag(2)′ = 3.438 (2) to Ag(1)···Ag(2)′ = Ag(1)′···Ag(2) = 4.315 (2) Å. The four silver atoms form a parallelogram with edges of 3.095 (1) and 4.315 (2) Å and a short diagonal of 3.438 (2) Å. All of these distances are best considered as nonbonding from electronic considerations, though the shortest ones of 3.095 Å are only 0.206 Å longer than the corresponding distance found in silver metal.

In contrast, the five iodine···iodine distances show considerably less variation than do the silver···silver distances, even though the two trends are reciprocal to each other: I(1)···I(2) = I(1)′···I(2)′ = 4.763 (1), I(1)···I(1)′ = 4.712 (2), and I(2)···I(1)′ = I(2)′···I(1) = 4.505 (1) Å.

The four silver–phosphorus bonds fall into two groups: those of trigonally coordinated silver atoms, viz., Ag(1)–P(1) = Ag(1)′–P(1)′ = 2.430 (3) Å, are somewhat shorter than those with tetrahedrally coordinated silver atoms Ag(2)–P(2) = Ag(2)′–P(2)′ = 2.454 (3) Å. The differences, though of some statistical significance, are much smaller than the variations manifested in the silver–iodine bond distances.

The I–Ag–I angles closely reflect the metal coordination number. Thus, I(1)–Ag(1)–I(2) of 118.90 (4)° is close to the ideal trigonal value of 120° while I(1)–Ag(2)–I(2), I(1)–Ag(2)–I(1)′, and I(2)–Ag(2)–I(1)′ of 109.13 (4), 107.79 (4), and 104.83 (4)°, respectively, are not far from the ideal tetrahedral value of 109.47°.

On the other hand, the Ag–I–Ag angles are highly acute with the exception of Ag(1)–I(1)–Ag(2)′ (99.82 (4)°). These small bridging angles of 67.43 (3), 64.41 (3), and 72.21 (4)° for Ag(1)–I(2)–Ag(2), Ag(1)–I(1)–Ag(2), and Ag(2)–I(1)–Ag(2)′, respectively, are most likely due to nonbonded repulsions between the halogen atoms.

One interesting difference between $(Ph_3P)_4Ag_4I_4$ (chair) and $(Ph_3P)_4Cu_4X_4$ (X = Br, I) is that, in the former, M(1)–X(1)–M(2)′ (99.82 (4)°) is smaller than X(2)–M(2)–X(1)′ (104.83 (4)°) while, in the latter two structures, the trend was reversed (i.e., 107.15 (7) vs. 102.32 (7)° for X = Br and 108.29 (7) vs. 104.20 (7)° for X = I). This reversal in trend may be attributed to the van der Waals repulsions between phenyl groups on P(1) and P(2)′ (or, equivalently, P(1)′ and P(2)) being enhanced in the latter clusters because of the smaller size of copper atoms (vide infra).

The two independent triphenylphosphines are normal. The six phosphorus–carbon bond lengths range from 1.793 (12) to 1.834 (11) Å (average 1.816 Å). The 36 carbon–carbon bond distances range from 1.293 (22) to 1.440 (19) Å (average 1.381 Å). The six Ag–P–C angles range from 108.6 (4) to 117.1 (4)° (average 113.7°) while the six C–P–C angles range from 104.1 (5) to 105.2 (5)° (average 104.9°). As in the cubane-like structure, the 12 P–C–C angles (cf. Table VII)

Table VII. Bond Angles (deg) with Esd's for $(Ph_3P)_4Ag_4I_4$ (Chair)

	A. Ag–I–Ag Angles		
Ag(1)–I(1)–Ag(2)	64.41 (3)	Ag(2)–I(1)–Ag(2)′	72.21 (4)
Ag(1)–I(1)–Ag(2)′	99.82 (4)	Ag(1)–I(2)–Ag(2)	67.43 (3)
	B. I–Ag–I Angles		
I(1)–Ag(1)–I(2)	118.90 (4)	I(1)–Ag(2)–I(2)	109.13 (4)
I(1)–Ag(2)–I(1)′	107.79 (4)	I(1)′–Ag(2)–I(2)	104.83 (4)
	C. P–Ag–I Angles		
I(1)–Ag(1)–P(1)	111.68 (8)	I(1)–Ag(2)–P(2)	104.54 (8)
I(2)–Ag(1)–P(1)	127.37 (9)	I(1)′–Ag(2)–P(2)	115.44 (8)
		I(2)–Ag(2)–P(2)	114.87 (8)
	D. P–Ag···Ag Angles		
P(1)–Ag(1)···Ag(2)	166.76 (9)	P(2)–Ag(2)···Ag(1)	127.60 (8)
P(1)–Ag(1)···Ag(2)′	130.26 (9)	P(2)–Ag(2)···Ag(1)′	91.08 (8)
		P(2)–Ag(2)···Ag(2)′	124.97 (9)
	E. Ag–P–C Angles		
Ag(1)–P(1)–C(1A)	117.10 (40)	Ag(2)–P(2)–C(1D)	114.49 (35)
Ag(1)–P(1)–C(1B)	108.61 (41)	Ag(2)–P(2)–C(1E)	112.54 (38)
Ag(1)–P(1)–C(1C)	115.14 (38)	Ag(2)–P(2)–C(1F)	114.39 (39)
	F. C–P–C Angles		
C(1A)–P(1)–C(1B)	104.5 (6)	C(1D)–P(2)–C(1E)	105.2 (5)
C(1A)–P(1)–C(1C)	105.3 (5)	C(1D)–P(2)–C(1F)	104.1 (5)
C(1B)–P(1)–C(1C)	105.1 (6)	C(1E)–P(2)–C(1F)	105.2 (5)
	G. P–C–C Angles		
P(1)–C(1A)–C(2A)	119.4 (9)	P(2)–C(1D)–C(2D)	117.0 (8)
P(1)–C(1A)–C(6A)	122.8 (11)	P(2)–C(1D)–C(6D)	122.2 (9)
P(1)–C(1B)–C(2B)	123.9 (11)	P(2)–C(1E)–C(2E)	116.4 (10)
P(1)–C(1B)–C(6B)	116.5 (10)	P(2)–C(1E)–C(6E)	123.5 (10)
P(1)–C(1C)–C(2C)	123.6 (9)	P(2)–C(1F)–C(2F)	117.2 (9)
P(1)–C(1C)–C(6C)	116.8 (9)	P(2)–C(1F)–C(6F)	122.7 (9)
	H. C–C–C Angles		
C(2A)–C(1A)–C(6A)	117.8 (13)	C(2D)–C(1D)–C(6D)	120.8 (11)
C(1A)–C(2A)–C(3A)	121.4 (12)	C(1D)–C(2D)–C(3D)	120.5 (11)
C(2A)–C(3A)–C(4A)	119.7 (15)	C(2D)–C(3D)–C(4D)	119.1 (13)
C(3A)–C(4A)–C(5A)	121.4 (16)	C(3D)–C(4D)–C(5D)	120.0 (14)
C(4A)–C(5A)–C(6A)	120.2 (16)	C(4D)–C(5D)–C(6D)	121.3 (13)
C(1A)–C(6A)–C(5A)	119.4 (15)	C(1D)–C(6D)–C(5D)	118.3 (12)
C(2B)–C(1B)–C(6B)	119.6 (13)	C(2E)–C(1E)–C(6E)	120.0 (12)
C(1B)–C(2B)–C(3B)	120.5 (15)	C(1E)–C(2E)–C(3E)	120.2 (14)
C(2B)–C(3B)–C(4B)	120.5 (19)	C(2E)–C(3E)–C(4E)	118.2 (16)
C(3B)–C(4B)–C(5B)	122.2 (19)	C(3E)–C(4E)–C(5E)	124.7 (17)
C(4B)–C(5B)–C(6B)	119.1 (17)	C(4E)–C(5E)–C(6E)	116.5 (15)
C(1B)–C(6B)–C(5B)	118.0 (14)	C(1E)–C(6E)–C(5E)	120.3 (13)
C(2C)–C(1C)–C(6C)	119.6 (11)	C(2F)–C(1F)–C(6F)	120.0 (11)
C(1C)–C(2C)–C(3C)	118.2 (11)	C(1F)–C(2F)–C(3F)	119.5 (11)
C(2C)–C(3C)–C(4C)	122.8 (13)	C(2F)–C(3F)–C(4F)	120.4 (13)
C(3C)–C(4C)–C(5C)	118.7 (14)	C(3F)–C(4F)–C(5F)	120.6 (13)
C(4C)–C(5C)–C(6C)	121.3 (15)	C(4F)–C(5F)–C(6F)	119.8 (12)
C(1C)–C(6C)–C(5C)	119.3 (13)	C(1F)–C(6F)–C(5F)	119.7 (12)
	I. CH_2Cl_2 Bond Angles		
Cl(1)–Cl(2)–Cl(4)	112 (2)	Cl(4)–Cl(2)–Cl(5)	136 (2)
Cl(2)–Cl(4)–Cl(3)	78 (1)	Cl(5)–Cl(2)–Cl(6)	110 (2)
		Cl(1)–Cl(2)–Cl(6)	85 (2)

can be divided into two groups: those oriented toward the Ag–P axis are greater than 120° (122.2 (9)–123.9 (11)°) whereas those oriented otherwise are smaller than 120° (116.4 (10)–119.4 (9)°), corresponding to the weak intratriphenylphosphine (Ph)H···H(Ph) repulsions among H(6A), H(2B), H(2C) in $Ph_3P(1)$ and H(6D), H(6E), H(6F) in $Ph_3P(2)$, respectively (cf. Table IXA).

The intra- and intermolecular van der Waals distances are listed in Table IX. The closest intramolecular nonbonding H(6A)···H(2C) distance of 2.70 Å is believed to be responsible for the large Ag(1)···Ag(2)′ = Ag(1)′···Ag(2) distances of 4.315 (2) Å mentioned above. Further implications of these nonbonding contacts will be discussed in the following section.

The solvent molecule, described here by six partial chlorine atoms of weights 0.329 (Cl(1)), 0.302 (Cl(2)), 0.359 (Cl(3)), 0.365 (Cl(4)), 0.327 (Cl(5)), and 0.089 (Cl(6)), is badly disordered and/or partially lost during the data collection. Each of these six partial chlorine atoms represents a chlorine and/or a carbon atom of the disordered solvent molecules. The most probable locations of the solvent molecules are Cl(1)–C(2)–Cl(4), Cl(4)–C(2)–Cl(5), Cl(2)–C(4)–Cl(3), Cl(5)–C(2)–Cl(6), and Cl(1)–C(2)–Cl(6) (cf. Tables VIG and VIIH).

The solvent molecules form weak hydrogen bondings with the $(Ph_3P)_4Ag_4I_4$ (chair) molecules via (1) I(1)···H–C(2) of 4.13 Å, (2) I(2)···H-C(4) of 4.05 Å, and (3) H(6B)···Cl(5) of 2.96 Å (cf. Table IXC).

II. Direct Comparison between the Cubane- and the Chair-like Forms. The observation of two isomers of $(Ph_3P)_4Ag_4I_4$ in the solid state provides an excellent opportunity for a direct comparison of the stereochemistries between the two forms.

First, the six Ag···Ag distances of 3.115–3.768 Å within the six highly nonplanar Ag_2I_2 faces of the cubane form are close

Table VIII. Nonbonding Contacts for $(Ph_3P)_4Ag_4I_4$ (Cubane)

A. Intramolecular I···H(Ph) (<3.80 Å) and (Ph)H···H(Ph′) (<2.85 Å) Contacts

I(1)···H(6A)	3.48	H(2A)···H(2B)	2.41
I(1)···H(6K)	3.60	H(5B)···H(3E)	2.49
I(2)···H(6J)	3.19	H(6B)···H(2E)	2.68
I(2)···H(6D)	3.74	H(6B)···H(3E)	2.75
I(3)···H(2I)	3.10	H(2D)···H(6E)	2.42
I(3)···H(2E)	3.17	H(5D)···H(5J)	2.80
I(3)···H(6D)	3.52	H(6I)···H(2J)	2.57
I(3)···H(6A)	3.78	H(2K)···H(2L)	2.83
I(4)···H(6L)	3.65	H(2L)···H(2M)	2.79
I(4)···H(6C)	3.67		
I(4)···H(6K)	3.67		

B. Intermolecular I···H(Ph) (<3.80 Å) and (Ph)H···H(Ph′) (<2.85 Å) Contacts

I(1)···H(4B)^{i} [a]	3.06	H(3C)···H(2H)^{iii}	2.32
I(1)···H(3A)^{ii}	3.32	H(4C)···H(3H)^{iii}	2.72
I(1)···H(4J)^{iii}	3.41	H(2D)···H(2M)^{xi}	2.75
I(1)···H(4A)^{ii}	3.56	H(3D)···H(2M)^{xi}	2.80
I(2)···H(4E)^{i}	2.95	H(5D)···H(3B)^{xii}	2.28
I(2)···H(4F)^{iv}	3.13	H(5E)···H(4K)^{xii}	2.51
I(2)···H(4K)^{v}	3.28	H(5E)···H(5K)^{xii}	2.71
I(4)···H(3L)^{vi}	3.26	H(5E)···H(4F)^{xi}	2.73
I(4)···H(4M)^{vii}	3.72	H(5E)···H(5L)^{xi}	2.81
I(4)···H(5M)^{vii}	3.72	H(6E)···H(5L)^{xi}	2.57
H(2A)···H(5A)^{viii}	2.62	H(2F)···H(5F)^{iv}	2.76
H(3A)···H(6H)^{viii}	2.83	H(5F)···H(3K)^{vi}	2.78
H(4A)···H(4J)^{ix}	2.47	H(6F)···H(4M)^{vii}	2.76
H(4A)···H(4B)^{ii}	2.82	H(3H)···H(5I)^{ix}	2.83
H(3B)···H(5D)^{x}	2.28	H(4H)···H(3J)^{ix}	2.68
H(3B)···H(5J)^{x}	2.75	H(2K)···H(3M)^{xiii}	2.48
H(3B)···H(4J)^{x}	2.83	H(3K)···H(3M)^{xiii}	2.67
H(5B)···H(6M)^{vii}	2.48		

[a] The superscripts refer to the following symmetry transformations: (i) $x, 1+y, z$; (ii) $2-x, {}^1/_2+y, {}^1/_2-z$; (iii) $x, {}^3/_2-y, -{}^1/_2+z$; (iv) $1-x, {}^1/_2+y, {}^1/_2-z$; (v) $x, {}^3/_2-y, {}^1/_2+z$; (vi) $1-x, 1-y, -z$; (vii) $x, -1+y, z$; (viii) $2-x, -{}^1/_2+y, {}^1/_2-z$; (ix) $2-x, 1-y, 1-z$; (x) $x, {}^1/_2-y, -{}^1/_2+z$; (xi) $1-x, -{}^1/_2+y, {}^1/_2-z$; (xii) $x, {}^1/_2-y, {}^1/_2+z$; (xiii) $1-x, 2-y, -z$.

Table IX. Nonbonding Contacts for $(Ph_3P)_4Ag_4I_4$ (Chair)

A. Intramolecular I···H(Ph) (<3.80 Å) and (Ph)H···H(Ph′) (<2.85 Å) Contacts

I(2)···H(3D)′ [a]	3.41	I(1)···H(6B)	3.58
I(2)···H(2A)	3.47	I(1)···H(2F)′	3.69
I(2)···H(2E)	3.62	I(1)···H(6C)	3.78
I(2)···H(2D)′	3.69	H(2A)···H(3D)′	2.77
I(1)···H(2D)	3.39	H(6A)···H(2C)	2.70

B. Intermolecular I···H(Ph) (<3.80 Å) and (Ph)H···H(Ph′) (<2.85 Å) Contacts

I(2)···H(4A)^{i} [a]	3.12	H(3A)···H(3D)^{vii}	2.36
I(2)···H(3B)^{ii}	3.25	H(3A)···H(3A)^{i}	2.51
I(2)···H(3F)^{iii}	3.31	H(4A)···H(4F)^{viii}	2.83
I(2)···H(4C)^{iv}	3.62	H(5A)···H(6D)^{viii}	2.47
I(2)···H(4F)^{iii}	3.70	H(5A)···H(5C)^{ix}	2.80
I(1)···H(5E)^{v}	3.17	H(6A)···H(5D)^{viii}	2.58
I(1)···H(4F)^{vi}	3.69	H(2C)···H(3C)^{x}	2.64
H(2A)···H(4B)^{ii}	2.34	H(2F)···H(3F)^{iii}	2.77
H(2A)···H(3A)^{i}	2.84	H(5F)···H(6F)^{xi}	2.58

C. Intermolecular I···Cl (<4.20 Å) and Cl···H(Ph) (<3.40 Å) Contacts between CH_2Cl_2 and $(Ph_3P)_4Ag_4I_4$

I(2)···Cl(4)^{iv} [a]	4.05 (2)	Cl(3)···H(2E)^{vi}	3.40
I(1)···Cl(2)	4.13 (2)	Cl(4)···H(2E)^{vi}	3.37
Cl(1)···H(6D)^{v}	3.30	Cl(5)···H(6B)	2.96
Cl(1)···H(2C)^{x}	3.38	Cl(5)···H(6E)^{v}	3.18
Cl(1)···H(6E)^{v}	3.35	Cl(6)···H(3B)^{x}	3.38
Cl(3)···H(2B)^{x}	3.30	Cl(6)···H(2E)^{vi}	3.21
Cl(3)···H(6F)^{v}	3.40	Cl(3)···H(6A)^{x}	3.37

[a] The superscripts refer to the following symmetry transformations: (prime) $1-x, -y, -z$; (i) $1-x, 1-y, -z$; (ii) $1-x, 1-y, 1-z$; (iii) $2-x, -y, -z$; (iv) $1+x, y, z$; (v) $1-x, -y, 1-z$; (vi) $-1+x, y, z$; (vii) $x, 1+y, z$; (viii) $-1+x, 1+y, z$; (ix) $-x, 1-y, -z$; (x) $-x, 1-y, 1-z$; (xi) $2-x, -y, 1-z$.

to the three Ag···Ag distances of 3.095–3.438 Å within the three Ag_2I_2 moieties but are substantially shorter than the two Ag(1)···Ag(2)′ distances of 4.315 Å across the bridge in the chair form. The much larger values of these latter two distances in comparison with the others signify the relief in intramolecular nonbonding repulsions between the phenyl groups of the phosphines attached to these two silver atoms (viz., Ag(1) and Ag(2)′ or Ag(1)′ and Ag(2)) in the chair-like isomer.

On the other hand, the six I···I distances of 4.399–4.801 Å in the cubane structure compare well with the five I···I distances of 4.505–4.763 Å in the chair form despite the fact that I(2)···I(1)′, which is the shortest iodine···iodine contact within the chair isomer, measures across the bridge joining the halves of the molecule. This smaller variation of iodine···iodine contacts (in comparison to the silver···silver distances), both within each isomer and on going from the cubane to the chair form, suggests that iodine···iodine nonbonded repulsions dictate to a significant extent the molecular parameters within each isomer but appears not to be the determining factor in the cubane → chair isomerization.

The 12 Ag–I distances in the cubane form, ranging from 2.836 to 3.037 Å, are close to that of 2.835–2.995 Å for the Ag(CN = 4)–I(CN = 3) distances but are in general longer than that of 2.724–2.849 Å for the Ag(CN < 4)–I(CN < 3) distances, in the chair isomer.

The Ag(CN = 4)–P distances of 2.455–2.462 Å in the cubane form agree with the Ag(CN = 4)–P distances of 2.454 Å but are somewhat longer than the Ag(CN = 3)–P distances of 2.430 Å in the chair form.

The intracluster angles also show interesting patterns. Within the cubane form, all Ag–I–Ag angles are acute (64.53–81.07°) whereas all I–Ag–I angles are obtuse (95.16–115.38°). A similar pattern is observed in the chair form except that the Ag(1)–I(1)–Ag(2)′ angle across the bridge is obtuse (99.82°). Furthermore, the I–Ag–I angles in the chair form reflect the coordination number of the silver atom (118.90° for CN = 3 and 104.83–109.13° for CN = 4).

A detailed comparison of van der Waals distances listed in Tables VIII and IX indicates *a significant relief in intramolecular nonbonding repulsions in going from the cubane to the chair isomer.* In fact, the shortest I···H distance of 3.39 Å and the shortest H···H distance of 2.70 Å (both greater than the van der Waals values) in the chair form are 0.29 Å larger than the corresponding values of 3.10 and 2.41 Å, respectively, in the cubane form. Within the unit cell, each cubane-like molecule occupies 1784 Å^3 (V/Z = 7137 Å^3/4) whereas each chair-like molecule occupies ca. 1846 Å^3 (1936 − 1.5 × 60). This expansion of the van der Waals volume of the molecule in going from the cubane to the chair form, along with the remarkable distortion of the cubane-like structure, strongly supports the premise that the cubane → chair isomerization is to a large extent caused by intramolecular nonbonded repulsions due to the overcrowding of the bulky triphenylphosphine and the bridging iodine ligands (vide infra).

An examination of the molecular parameters revealed that one of the six highly nonplanar Ag_2I_2 moieties (namely, Ag(1)I(3)Ag(3)I(4)) in the cubane-like structure resembles the nonplanar Ag_2I_2 (i.e., Ag(1)I(2)Ag(2)I(1)) fragment in the chair-like isomer. This resemblance is evident from the fact that each of these two nonplanar faces possesses the shortest Ag···Ag distances of 3.115 (2) and 3.095 (1) Å and the longest I···I contacts of 4.801 (2) and 4.763 (1) Å in the cubane- and the chair-like configuration, respectively. As a result, the Ag–I–Ag angles are also very similar in magnitude (viz., Ag(1)–I(3)–Ag(3) of 64.53 (4)° and Ag(1)–I(4)–Ag(3) of 65.93 (5)° in the cubane and Ag(1)–I(2)–Ag(2) of 67.43 (3)° and Ag(1)–I(1)–Ag(2) of 64.41 (3)° in the chair form), both being the smallest within each cluster. The main difference between the two faces, however, is that in the former

the two silver atoms are approximately tetrahedral-coordinated, while in the latter one silver atom is approximately tetrahedral-coordinated and the other is approximately trigonal-coordinated. This difference causes the two silver–iodine bonds formed by the trigonally coordinated silver atom to be significantly shorter than the other two in the chair form.

The point of interest is that three of the four longest Ag–I bonds in the cubane-like isomer, viz., Ag(1)–I(1), Ag(4)–I(4), and Ag(2)–I(3), are approximately normal to the nonplanar face Ag(1)I(3)Ag(3)I(4). Assuming that the longest bonds are most susceptible to cleavage in the course of isomerization, it is apparent that rupture of any two of these Ag–I bonds, followed by a rotation of ca. 180° of the face opposite to Ag(1)I(3)Ag(3)I(4), will lead to the chair form. If this concerted mechanism (possibly triggered by solvation) is correct, the existence of a boat form which acts as an intermediate in the isomerization process must be postulated. The conversion of the boat to the chair form, however, requires configuration inversion at the Ag–I bond about which the rotation takes place. On the other hand, we cannot rule out other plausible pathways which include the dissociation of the cubane isomer into two dimers followed by the recombination of the dimers to form the chair isomer.

III. Factors Influencing Cubane ⇌ Chair Isomerization or Cubane → Chair Conversion. From a detailed comparison of the stereochemistries among the series $(Ph_3P)_4Ag_4X_4$ as well as with their copper analogues $(Ph_3P)_4Cu_4X_4$, $(Et_3P)_4Cu_4X_4$, and $(Et_3As)_4Cu_4I_4$ primarily due to Churchill and coworkers,[12] we are led to the conclusion that the stereochemical variations, which manifest themselves in (1) undistorted cubane-like structure in $(Et_3P)_4Cu_4X_4$ and $(Et_3As)_4Cu_4I_4$, (2) the distortion of a cubane-like structure in $(Ph_3P)_4Ag_4X_4$ and $(Ph_3P)_4Cu_4Cl_4$, (3) cubane ⇌ chair isomerism in $(Ph_3P)_4Ag_4I_4$, and (4) conversion to the chair-like configuration in $(Ph_3P)_4Cu_4X_4$ (X = Br, I), must be to a significant extent due to intramolecular nonbonded interactions. These latter interactions are dependent upon the size of the metal (M), the bridging halogen (X), the terminal pnicogen (Y), and the terminal ligand substituents (R) in the following ways. As (1) the covalent radii of the metal atoms decrease (e.g., Ag > Cu), (2) the sizes of the bridging halogen atoms increase (e.g., Cl < Br < I), (3) the terminal pnicogen atoms get smaller (e.g., As > P), or (4) the organic R groups become bulkier (e.g., alkyl < phenyl), the steric repulsions of the types M···M, X···X, R···R, and R···X are enhanced. Though these nonbonded interactions are mutually interdependent, it is evident from the known data that the latter two are primarily responsible for the distortion of the cubane-like molecules from the optimal T_d geometry. The degree of distortion generally follows the degree of steric hindrance. For example, the distortion of $(Ph_3P)_4Ag_4I_4$ (cubane-like) is much more severe than that of the corresponding chloride or bromide; similarly, $(Et_3P)_4Cu_4X_4$ conforms to the precise T_d symmetry as opposed to $(Ph_3P)_4Cu_4Cl_4$ which has a markedly distorted cubane-like structure. As this steric strain becomes unusually severe, the molecule eventually isomerizes as in the case of $(Ph_3P)_4Ag_4I_4$ or converts as in the case of $(Ph_3P)_4Cu_4X_4$, X = Br, I, to a chair-like structure.

A somewhat more quantitative measure of the steric hindrance of the type R···X within the $(R_3Y)_4M_4X_4$ molecule is the overlap of the van der Waals sphere of the bridging ligand X with the cone angle of the terminal ligand R_3Y. Using the estimated cone angle[31] of 145° for a triphenylphosphine ligand and the observed average M–X distances and average Y–M–X angles, Figure 5 shows such an effect for the cubane-like series $(Ph_3P)_4Ag_4X_4$ and $(Ph_3P)_4Cu_4X_4$ (X = Cl, Br, I). For the copper systems, the curves labeled with primes refer to the hypothetical cubane-like structure based upon the Cu–X

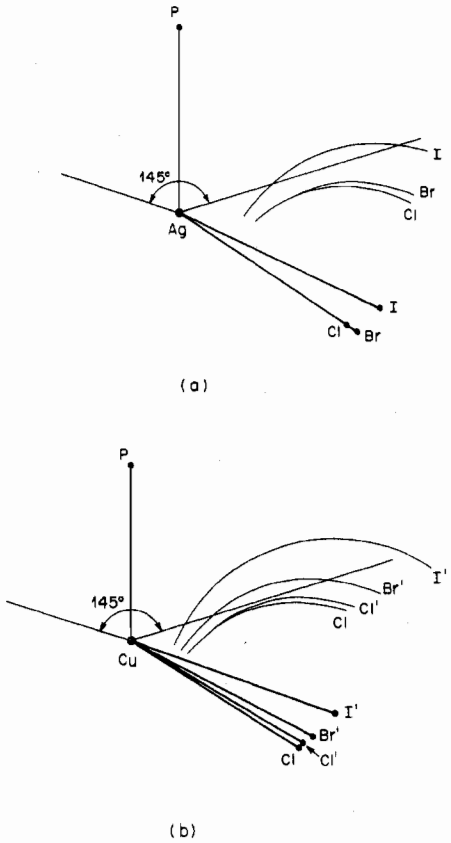

Figure 5. Steric overlap of the cone angle (145° [31]) of Ph_3P and the van der Waals sphere[27] of X. (a) $(Ph_3P)_4Ag_4X_4$: Ag–X = 2.653, 2.800, 2.910 Å, P–Ag–X = 122.35, 122.32, 114.11° for X = Cl, Br, I, respectively.[11] (b) $(Ph_3P)_4Cu_4Cl_4$: Cu–Cl = 2.444 Å, P–Cu–Cl = 122.02°; the curves labeled with primes are for hypothetical cubane-like structures of $(Ph_3P)_4Cu_4X_4$ based upon Cu–X = 2.438, 2.544, 2.684 Å and P–Cu–X = 120.02, 116.80, 109.56° for X = Cl, Br, I, respectively, observed in the cubane-like $(Et_3P)_4Cu_4X_4$ molecules.[12]

distances and the P–Cu–X angles observed in the corresponding cubane-like $(Et_3P)_4CuX_4$ clusters. It is apparent from Figure 5a that the (Ph)H···X type nonbonded repulsions in the $(Ph_3P)_4Ag_4X_4$ species do not occur until X = I. Indeed, we observe to date the cubane ⇌ chair isomerization only for $(Ph_3P)_4Ag_4I_4$. On the other hand, the steric repulsions of the type (Ph)H···X increase significantly from $(Ph_3P)_4Cu_4Cl_4$ to $(Ph_3P)_4Cu_4Br_4$ and $(Ph_3P)_4Cu_4I_4$ as shown in Figure 5b, in accord with the observation of Churchill et al. that $(Ph_3P)_4Cu_4Cl_4$ possesses a distorted cubane-like structure whereas each of $(Ph_3P)_4Cu_4X_4$ (X = Br, I) adopts a chair-like configuration in the solid state.

In conclusion, as the steric hindrance among the ligands increases, the following stereochemical variation inevitably occurs

symmetrical "cubane" → distorted "cubane" → ("cubane" ⇌ "chair" isomerization) → "chair"

Figure 6 summarizes such a stereochemical pattern for $(Ph_3Y)_4M_4X_4$. For the structurally yet unknown $(Ph_3As)_4Cu_4X_4$ series we predict that the cubane → chair isomerism or conversion will take place somewhere between the $(Ph_3P)_4Ag_4X_4$ and the $(Ph_3P)_4Cu_4X_4$ series, i.e., in the vicinity of $(Ph_3As)_4Cu_4Br_4$.

IV. Ionicity vs. Covalency—a Weak Link between $(R_3Y)_4M_4X_4$ and MX? Spectroscopic ionicity was believed to be the predominant factor in dictating the tetrahedral–octahedral transformation in solid electrolytes such as argentous halide and cuprous halide. It has been shown by

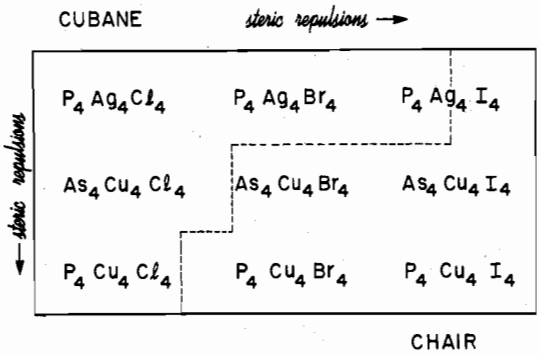

Figure 6. Stereochemical behavior of the $(Ph_3Y)_4M_4X_4$ (Y = P, As; M = Cu, Ag; X = Cl, Br, I) molecules.

Phillips[32] and others[33] that as the ionicity increases along the sequence CuI (0.692), CuBr (0.735), CuCl (0.746), AgI (0.770), AgBr (0.850), and AgCl (0.856), the tendency to form the more ionic rock salt (NaCl) structure with octahedral coordination as opposed to the more covalent zinc blende or wurzite structure with tetrahedral coordination increases. Thus, at STP, AgCl and AgBr adopt the former structure whereas AgI and CuX adopt the latter structure. Near the characteristic ionicity of 0.785, AgI can easily be transformed from the tetrahedral to the octahedral structure, with the energy difference being only $\lesssim$0.5 kcal/mol.

A cubane-like molecular structure of $(R_3Y)_4M_4X_4$ type can be considered as derived from the rock salt lattice of MX by taking one-eighth of the unit cell and embedding it in the tetrahedral array of the terminal ligands (or more precisely, Y). In such a formal transformation, however, the coordination number of the metal atoms changes from six (in the rock salt structure) to four which is similar to that in the zinc blende or wurzite structure. Hence, we believe the formation of a cubane-like $(R_3Y)_4M_4X_4$ molecule from the MX lattice is formally analogous to the rock salt → (zinc blende or wurzite) transition in that it increases significantly the covalency of the cluster core. In this context, it should be noted that in the $(R_3Y)_4M_4X_4$ series, the M–X bond lengths lie somewhere between the extremes expected for covalent and ionic bonds whereas the M–Y bond lengths fall into the normal covalent range.

Similar argument can be applied to the chair-like structure. And, *there seems to be a general correlation between the covalency in the parent MX and the tendency favoring a chair-like over a cubane-like structure.* The apparent exception, of course, is $(Ph_3P)_4Cu_4Cl_4$ which has a cubane-like configuration. In fact, the ease of cubane ⇌ chair isomerization in $(Ph_3P)_4Ag_4I_4$ coincides with the ease of zinc blende ⇌ rock-salt transition in AgI. This qualitative analogy apparently stems from the small energy difference between tetrahedral and trigonal coordinations in $(Ph_3P)_4M_4X_4$ and between tetrahedral and octahedral coordinations in MX, especially when the ionicity approaches the characteristic value of 0.785 (i.e., longer, more numerous, and more ionic bonds in higher coordination lie close in energy to shorter, less numerous, and more covalent bonds in lower coordination).

However, on account of the fact that all $(Et_3Y)_4M_4X_4$ species known to date adopt a cubane-like structure, we maintain that intramolecular van der Waals interactions play a determinative role in dictating the molecular structure of the $(R_3Y)_4M_4X_4$ cluster family, providing that the ionicity of the M–X bond lies close to the critical value separating sphalerite and rock salt structures.

Furthermore, the fact that $(Ph_3P)_4Ag_4I_4$ represents the first determined metal cluster which can exist in both cubane and chair forms in the solid state suggests that these forms are fairly close in energy with the difference being comparable to van der Waals interactions (as well as solvation or crystal packing).

Registry No. $[(C_6H_5)_3PAgI]_4$, 54937-07-4; $[(C_6H_5)_3PAgI]_4 \cdot 1.5CH_2Cl_2$, 59765-79-6.

Supplementary Material Available: Tables of observed and calculated structure factors for the cubane and the chair isomers of $(Ph_3P)_4Ag_4I_4$ (40 pages). Ordering information is given on any current masthead page.

References and Notes

(1) (a) Bell Laboratories. (b) University of Wisconsin.
(2) (a) M. A. Neuman, Trinh-Toan, and L. F. Dahl, *J. Am. Chem. Soc.*, **94**, 3383 (1972); (b) Trinh-Toan, W. P. Fehlhammer, and L. F. Dahl, *ibid.*, **94**, 3389 (1972).
(3) (a) C. H. Wei, G. R. Wilkes, P. M. Treichel, and L. F. Dahl, *Inorg. Chem.*, **5**, 900 (1966); (b) R. A. Schunn, C. J. Fritchie, Jr., and C. T. Prewitt, *ibid.*, **5**, 892 (1966).
(4) (a) Trinh-Toan, W. P. Fehlhammer, and L. F. Dahl, to be submitted for publication; (b) Trinh-Toan, B. K. Teo, W. P. Fehlhammer, and L. F. Dahl, to be submitted for publication.
(5) (a) G. L. Simon and L. F. Dahl, *J. Am. Chem. Soc.*, **95**, 2175 (1973); (b) G. L. Simon and L. F. Dahl, *ibid.*, **95**, 2164 (1973).
(6) (a) R. S. Gall, C. T.-W. Chu, and L. F. Dahl, *J. Am. Chem. Soc.*, **96**, 4019 (1974); (b) R. S. Gall, N. G. Connelly, and L. F. Dahl, *ibid.*, **96**, 4017 (1974).
(7) (a) B. K. Teo, Ph.D. Thesis, University of Wisconsin, 1973; (b) B. K. Teo and L. F. Dahl, to be submitted for publication.
(8) (a) B. A. Averill, T. Herskovitz, R. H. Holm, and J. A. Ibers, *J. Am. Chem. Soc.*, **95**, 3523 (1973); (b) L. Que, Jr., M. A. Bobrik, J. A. Ibers, and R. H. Holm, *ibid.*, **96**, 4168 (1974); (c) C. Y. Yang, K. H. Johnson, R. H. Holm and J. G. Norman, Jr., *ibid.*, **97**, 6596 (1975).
(9) J. A. Bertrand, A. P. Ginsberg, R. I. Kaplan, C. E. Kirkwood, R. L. Martin, and R. C. Sherwood, *Inorg. Chem.*, **10**, 240 (1971).
(10) (a) A. F. Wells, *Z. Kristallogr., Kristallgeom., Kristallphys., Kristallchem.*, **94**, 447 (1936); (b) F. G. Mann, D. Purdie, and A. F. Wells, *J. Chem. Soc.*, 1503 (1936); (c) F. G. Mann, A. F. Wells, and D. Purdie, *ibid.*, 1828 (1937).
(11) (a) A preliminary account of this work has appeared in B. K. Teo and J. C. Calabrese, *J. Am. Chem. Soc.*, **97**, 1256 (1975). (b) B. K. Teo and J. C. Calabrese, *Inorg. Chem.*, preceeding paper in this issue. (c) B. K. Teo and J. C. Calabrese, *J. Chem. Soc., Chem. Commun.*, 185 (1976).
(12) (a) M. R. Churchill and K. L. Kalra, *Inorg. Chem.*, **13**, 1899 (1974); (b) M. R. Churchill, B. G. Deboer, and S. J. Mendak, *ibid.*, **14**, 2041 (1975); (c) M. R. Churchill and K. L. Kalra, *ibid.*, **13**, 1065 (1974); (d) M. R. Churchill and K. L. Kalra., *ibid.*, **13**, 1427 (1974); (e) M. R. Churchill, B. G. Deboer, and D. J. Donovan, *ibid.*, **14**, 617 (1975); (f) M. R. Churchill and B. G. Deboer, *ibid.*, **14**, 2502 (1975).
(13) W. R. Clayton and S. G. Shore, *Cryst. Struct. Commun.*, **2**, 605 (1973).
(14) (a) N. Marsich, G. Nardin, and L. Randaccio, *J. Am. Chem. Soc.*, **95**, 4053 (1973); (b) G. Nardin and L. Randaccio, *Acta Crystallogr., Sect. B*, **30**, 1377 (1974); (c) A. Camus, G. Nardin, and L. Randaccio, *Inorg. Chim. Acta*, **12**, 23 (1975).
(15) "International Tables for X-Ray Crystallography", Vol. I, 2d ed, Kynoch Press, Birmingham, England, 1965: (a) p 99; (b) p 75.
(16) R. A. Sparks et al., "Operations Manual. Syntex P1 Diffractometer", Syntex Analytical Instruments, Cupertino, Calif., 1970.
(17) The absorption correction program DEAR (J. F. Blount) uses the Gaussian integration method of W. R. Busing and H. A. Levy, *Acta Crystallogr.*, **10**, 180 (1957).
(18) The integrated intensity (I) was calculated according to the expression $I = [S - (B_1 + B_2)/B_R]T_R$ where S is the scan counts, B_1 and B_2 are the background counts, B_R is the ratio of background time to scan time, and T_R is the 2θ scan rate in degrees per minute. The standard deviation of I was calculated as $\sigma(I) = T_R[S + (B_1 + B_2)/B_R^2 + (pI)^2]^{1/2}$.
(19) All least-squares refinements were based on the minimization of $\sum w_i||F_o| - |F_c||^2$ with the individual weights $w_i = 1/\sigma(F_o)^2$.
(20) Atomic scattering factors used for all nonhydrogen atoms are from H. P. Hanson, F. Herman, J. D. Lea, and S. Skillman, *Acta Crystallogr.*, **17**, 1040 (1964); those for the hydrogen atoms are from R. F. Stewart, E. R. Davidson, and W. T. Simpson, *J. Chem. Phys.*, **42**, 3175 (1965).
(21) Hydrogen atoms were calculated at C–H distances of 1.00 Å and assigned constant isotropic thermal parameters of 7.00 Å^2.
(22) For other crystallographic details see T. H. Whitesides, R. W. Slaven, and J. C. Calabrese, *Inorg. Chem.*, **13**, 1895 (1974).
(23) $R_1 = [\sum||F_o| - |F_c||/|F_o|] \times 100\%$ and $R_2 = [\sum w_i||F_o| - |F_c||^2/\sum w_i|F_o|^2]^{1/2} \times 100\%$. See supplementary material for a listing of observed and calculated structure factors.
(24) "International Tables for X-Ray Crystallography", Vol. III, Kynoch Press, Birmingham, England, 1962, p 215.
(25) C. K. Johnson, *J. Appl. Crystallogr.*, **6**, 318 (1973): ORTEP2.
(26) *Chem. Soc., Spec. Publ.*, **No. 18**, S3s (1965).
(27) van der Waals radii of Cl (1.80 Å), Br (1.95 Å), and I (2.15 Å), are taken from L. Pauling, "The Nature of the Chemical Bond", 3d ed, Cornell University Press, Ithaca, N.Y., p 260.
(28) The following estimated single-bond covalent radii were taken from L. Pauling, "The Nature of the Chemical Bond", 3d ed, Cornell University

Press, Ithaca, N.Y., 1960, pp 224, 256: Cl, 0.99 Å; Br, 1.14 Å; I, 1.33 Å; P, 1.10 Å; As, 1.21 Å; Cu, 1.17 Å; Ag, 1.34 Å.
(29) (a) R. W. G. Wyckoff, "Crystal Structures", Vol. 1, Interscience, New York, N.Y., 1963, pp 110, 186; (b) V. H.-J. Meyer, *Acta Crystallogr.*, **16**, 788 (1963); (c) C. J. Gilmore, P. A. Tucker, and P. Woodward, *J. Chem. Soc. A*, 1337 (1971); (d) S. Geller, *Science*, **157**, 310 (1967); (e) S. Geller and M. D. Lind, *J. Chem. Phys.*, **52**, 5854 (1970).
(30) L. F. Dahl, E. Rodulfo de Gil, and R. D. Feltham, *J. Am. Chem. Soc.*, **91**, 1653 (1969).
(31) C. A. Tolman, *J. Am. Chem. Soc.*, **92**, 2956 (1970).
(32) (a) J. C. Phillips, *Rev. Mod. Phys.*, **42**, 317 (1970); (b) A. Navrotsky and J. C. Phillips, *Phys. Rev. B*, **11**, 1583 (1975); (c) J. C. Phillips, *J. Electrochem. Soc.*, **123**, 934 (1976).
(33) J. S. John and A. N. Bloch, *Phys. Rev. Lett.*, **33**, 1095 (1974).

Contribution from the Department of Chemistry, University of California, Irvine, California 92717

Crystal and Molecular Structure of a Ruthenium Complex Containing a Metalated Perfluoroazobenzene Ligand and a Novel 2-(η-Cyclopentadienyl)phenyl Group

JAMES A. MORELAND and ROBERT J. DOEDENS*

Received April 2, 1976 AIC60247E

The product of the reaction of decafluoroazobenzene with $Ru(CH_3)(PPh_3)_2(\eta\text{-}C_5H_5)$ has been shown by a crystal structure analysis to have an unusual structure. Crystals of (diphenyl(2-(η-cyclopentadienyl)phenyl)phosphine)(nonafluoro(phenylazo)phenyl-C^2,N')ruthenium are monoclinic, space group $P2_1/c$, with four molecules in a unit cell of dimensions a = 15.650 (14) Å, b = 13.338 (11) Å, c = 14.741 (11) Å, and β = 97.38 (3)°. The structure determination was based upon 3092 independent nonzero diffraction maxima with $2\theta < 45°$ collected by counter methods. A blocked full-matrix least-squares refinement converged to a final conventional discrepancy factor of 0.046. The molecule contains not only the expected metalated perfluoroazobenzene ligand but also a linkage between the η-cyclopentadienyl group and one of the phenyl rings of the triphenylphosphine. The resulting σ,π chelating configuration causes the substituted cyclopentadienyl ring to be tilted by ~13° relative to the ML_3 portion of the molecule. The fluorinated azobenzene ligand is bound in a chelating fashion via Ru–C and Ru–N bonds. The free phenyl ring is twisted by 64.6° from from the chelate plane. Bond distances involving this ligand include Ru–N = 2.020 (5) Å, Ru–C = 2.013 (6) Å, and N–N = 1.310 (7) Å.

Introduction

The ortho metalation of azobenzene, first reported about 10 years ago,[1] has proven to be the prototype of an extensive and important series of chemical reactions.[2-4] These reactions typically involve formation of a metal–carbon σ bond to an aromatic ring, with the displaced hydrogen atom either being eliminated or remaining bound to the metal atom. It is generally believed that the metalation of azobenzene proceeds by a pathway involving initial metal coordination of the azo group, followed by intramolecular attack upon the aromatic ring remote from the bound nitrogen atom.[2] Studies of the metalation of substituted azobenzenes by $PdCl_4^{2-}$ strongly suggested an electrophilic mechanism for the intramolecular metalation process in this case.[5,6] However, it has been suggested that under other circumstances (e.g., electron-rich metal atoms, azobenzenes with electron-withdrawing substituents) metalation could occur by a nucleophilic pathway.[7] This hypothesis has found support in studies of the metalation reaction of 3-monofluoroazobenzene with $CH_3Mn(CO)_5$, where the predominant product is the isomer which would be favored by a nucleophilic mechanism.[6]

In view of these results, the reactions of polyfluorinated azobenzenes, which should be susceptible to nucleophilic attack, with various transition metal systems have been investigated[8,9] in order to determine whether metalation can occur by fluorine abstraction from these ligands. From the reaction of $Ru(CH_3)(PPh_3)_2(\eta\text{-}C_5H_5)$ with decafluoroazobenzene, a product was obtained whose ^{19}F NMR spectrum was that expected of a metalated $C_6F_5N_2C_6F_4$ ligand but whose ^1H NMR spectrum suggested that substitution had also occurred on the cyclopentadienyl ring.[9] We now report results of a crystal structure analysis of this product, which confirms the proposed metalated structure and demonstrates that an unusual type of linkage has been formed between the cyclopentadienyl group and one of the phenyl rings of the triphenylphosphine ligand. These results have previously appeared in preliminary form.[10]

Table I

A. Crystal Data

Formula	$RuC_{35}F_9H_{18}N_2P$	V	3051.5 Å^3
Fw	769.57	Z	4
a	15.650 (14) Å	d(obsd)	1.70 (5) g/cm^3
b	13.338 (11) Å	d(calcd)	1.68 g/cm^3
c	14.741 (11) Å	Space group	$P2_1/c$
β	97.38 (3)°	μ(Mo Kα)	6.5 cm^{-1}

B. Experimental Parameters

Radiation	Mo Kα, λ(Kα_1) 0.709 30 Å, 3.0-mil Nb filter	Scan range	−0.65 + 0.60° in 2θ from Kα_1 peak
Temp	23 °C	Background counting	20-s fixed counts at each end of scan
Receiving aperture	5 × 5 mm, 29 cm from crystal		
Takeoff angle	2.1°	2θ(max)	45°
		Data collected	4135
Scan rate	1.0°/min in 2θ	Data with $F_o^2 > 3\sigma(F_o^2)$	3092

Experimental Section

Data Collection and Reduction. A suitably crystalline sample of the title compound was supplied by Dr. M. I. Bruce. Preliminary precession photographs showed monoclinic symmetry with systematic absences ($h0l$, $l \neq 2n$; $0k0$, $k \neq 2n$) uniquely defining space group $P2_1/c$. Cell parameters were obtained by least-squares refinement of the setting angles of 13 reflections which had been accurately centered on a Picker four-circle x-ray diffractometer.[11] Owing to the solubility of the crystals in many solvents and to the limited amount of sample available, only an approximate value of the observed density could be determined by flotation methods. Crystal data are tabulated in part A of Table I.

Intensity data were collected from a dark green thin platelet of dimensions 0.09 × 0.23 × 0.38 mm mounted approximately along the crystallographic b axis. Bounding planes belonged to the {100}, {010}, {001}, and {110} forms. Narrow-source, open-counter ω scans through several reflections displayed an average full width at half-